IEA Wind Task 42

Lifetime Extension Assessment

Deliverable Report 5+6: Data driven life prediction & comparison

December 2022

René Meklenborg and Lasse Svenningsen (section 1, 3)

EMD A/S

Clemens Hübler (section 4)

University of Hannover

Andreas Vad and Anik Hirenkumar Shah (section 5)

Technical University of Munich

Asger Bech Abrahamsen and Athanasios Kolios (section 1, 2)

Technical Univesity of Denmark

Stavroula Tsiapoki (section 6)

Wölfel

Contents

1 Introduction

The historic expansion of the global installed wind turbine capacity by 2021 is shown in Figure 1 and is illustrating that 1 TW will soon be reached (Lee & Zhao, 2022). The figure is however also showing that about 24-31 GW was installed 20 years, which is equal to the the design life time of onshore wind turbines as specified by the IEC 61400-1 standard (IEC, 2019). Thus the global wind turbine capacity that has allready undergone a decision about life extension is in the order of 30 GW. The average wind turbine rating instaled around 2001 was in the order of 1-2 MW and this is showing that the 30 GW capacity older than 20 years corresponds to several 10000 tubines involved in life extension operations.

A large number of owners therefore face the difficult decision whether to repower, decommission or lifetime extend their assets and the capacity involved in life extension operations will increase to about 200 GW over the next 10 years according to Figure 1. To make sure that the most economically feasible solutions are chosen it is essential that relevant information gathered at the wind farms is used to support this decision process.

To assess the remaning fatigue lifetime of a wind turbine, the DNV GL guideline (DNVGL-ST-0262, 2016) lists three assessment methods,

(i) analytical (simulation),

(ii) practical (inspection),

(iii) data-driven methods (measurements).

This report focuses on the third data-driven method, which may be divided into four sub-categories (Megavind, 2016):

(i) no design basis or operational measurement available,

(ii) design basis without any operational measurements,

(iii) design basis with SCADA based measurements,

(iv) design basis with multilayer load and operational measurements.

Data driven assessments in categories (iii) and (iv) give the most accurate assessments but also requires significantly more data compared to the first two categories.

In the following sections four methods are presented which also represent the subcategories of data-driven methods. The methods are then compared in terms of needed input, provided output, and limitations and benefits associated to the required data for the methods to work.

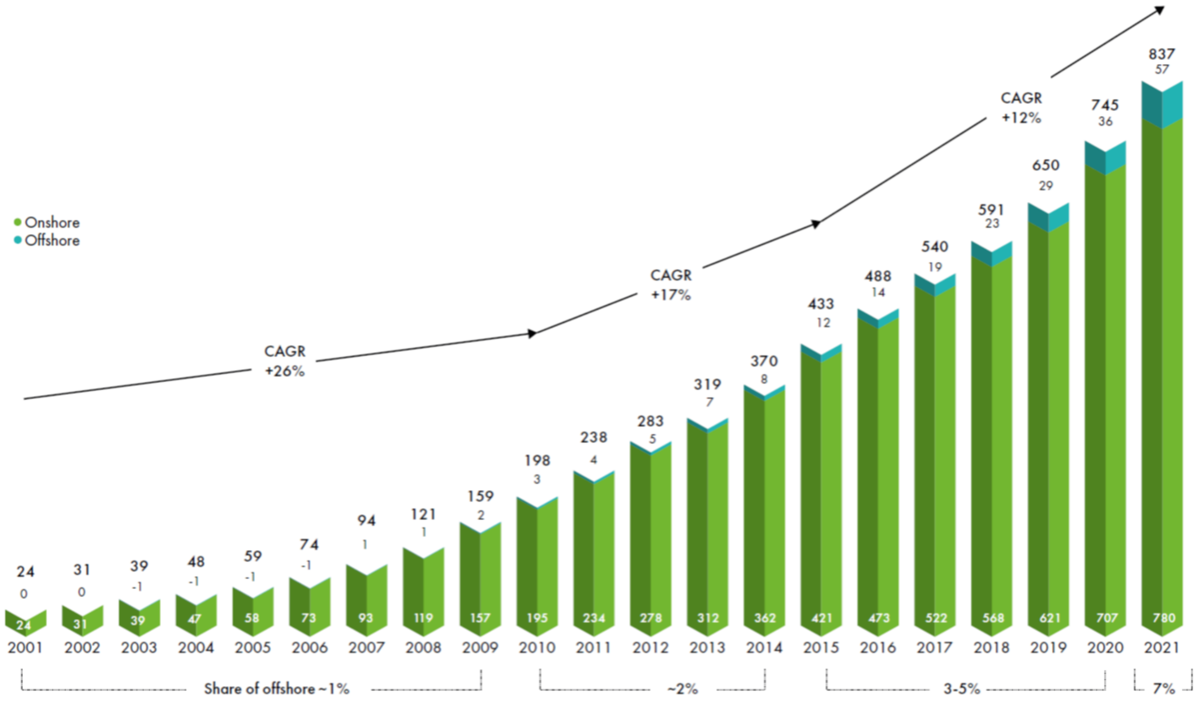

Figure 1 Historic development of the Global installed wind energy capacity [GW] from 2001 and to 2021 as reported by the Global Wind Energy Council(GWEC) in 2022. The global capacity older than the 20 year design life time of onshore wind turbine is seen to be about 30 GW and these turbines will be involved in life extension decisions. Reproduced from (Lee & Zhao, 2022).

2 Data

The IEA Task 42 Life extension workpackage 1 has indentified a number of wind turbine test cases to be used to demonstarte methods for evaluating the consumed life time and the possible remaining usefull life time of the turbines. The cases range from a single onshore wind turbine and to both on- and offshore wind farms as presented in the following sections. A benchmarking of the different methods using the same cases was originally intended for the deliverable report, but legal restiction of data and model sharing has made this task unfeasible. Future work on establishing data sets for such open comparisons is suggested for the possible extension of the IEA task 42.

2.1. Vestas V52 research turbine at DTU Risø Campus

DTU Wind and Energy Systems has a Vestas V52 wind turbine installed at the DTU Risø campus near the town Roskilde in Denmark as shown in Figure 2. This turbine is owned and operated by Technical University of Denmark(DTU) with the intension to used it for performing research projects, where measurement systems such a LIDARS can be mounted on the turbine nacelle in order to map the incomming wind field or the wake created behind the turbine. The V52 research turbine of DTU is position in the so called turbine row at the DTU Wind and Energy Systems test site, where met masts are installed in front of the turbine test sites in order to measure the incomming wind. The V52 research turbine and the met mast is shown in Figure 2.

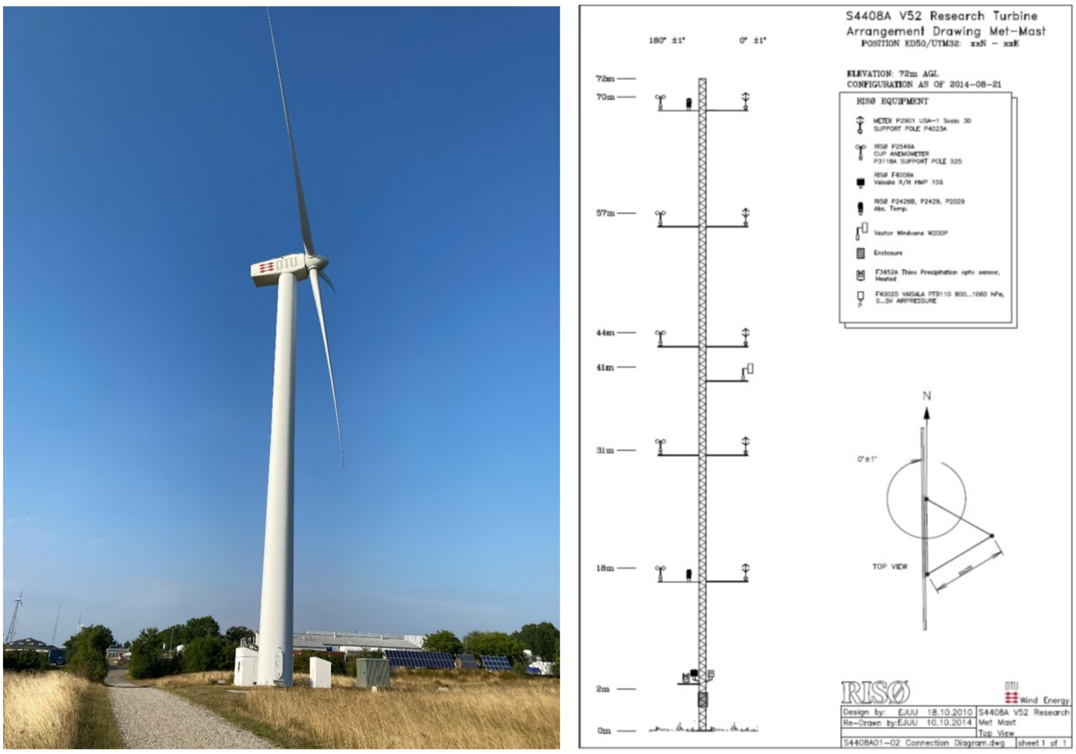

*Figure 2 **Left**: The DTU research Vestas V52 turbine at the DTU Risø campus near the city Roskilde in Denmark. **Right**: The meteorology mast measuring the incoming wind conditions*

in front and east of the V52 turbine (reproduced from (Paulsen, Gomiero, Larsen, & Benini, 2018)).

The specifications of the V52 research turbine are listed in Table 1.

Table 1 Specifications of V52 research turbine at DTU Risø Campus.

Manufacturer :	**Vestas**	**V52 – 850 kW**	**Installed : 2015**
Rated power	850 kW	**Rotor diameter**	52 m
Rated wind speed	16 m/s	**Tip / Hub height**	70 m / 44 m
Cut-in wind speed	4 m/s	**Blades**	3 pitch regulated
Cut-out wind speed	25 m/s	**Gearbox**	1 planet + 2 helical
Rotation speed	14-31.4 rpm	**Generator**	Double fed induction

The position of the DTU Risø Campus is about 30 km east from Copenhagen the capital of Denmark and is facing Roskilde fjord as shown Figure 3. It can be seen that that the average annual wind speed at the DTU Risø Campus is about 7 m/s at about 50 m height, which is considerable smaller than the wind speeds observed at the coast line facing the North sea. The position of the V52 research turbine and the met mast in the turbine test row at the DTU Risø Campus is shown in Figure 3 right. It can be seen that the turbine test row is facing a fjord to the east and that the surface elevation of the V52 research turbine is about 10 m above sea level.

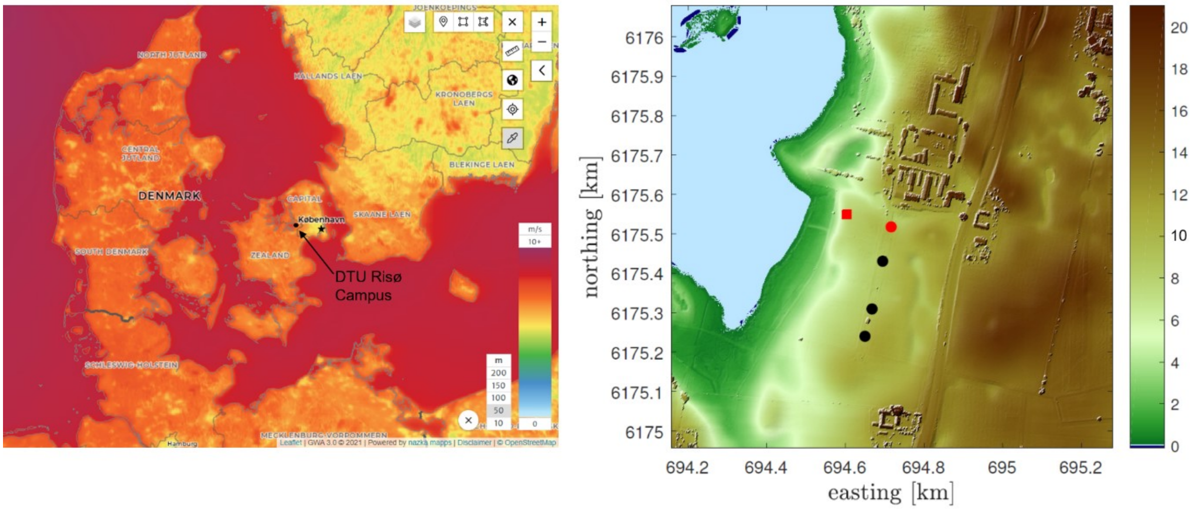

Figure 3 ***Left****: Map of Denmark showing the position of the DTU Risø Campus and the average annual wind speed at 50 m height as given by the Global Wind Atlas.* ***Right****: Digital surface elevation model in the units of UTM32 WGS84 and [m] of the turbine row at the DTU Risø Campus. The V52 research turbine is marked with the red circle and the met mast in front of the turbine is marked with the red square. Other turbines are positioned at the black dots. Reproduced from (Peña, Mann, & Rolighed Thorsen, 2018)).*

The V52 research turbine of DTU has been instrumented with a large number of sensors additional to the sensors of the Supervisory Control And Data Acquisition (SCADA) system of the turbine. The additional sensors are logged along with the SCADA data in a central data base holding also the synchronized wind speed measurements of the V52 met mast. Table 2 is showing how strain gauges were added to the blades in order to measure the blade deflections at the blade root. Strain gauges have also been mounted in at the tower base and are sampled at a freqeuncy of 35 Hz. One challenge of using strain gauges for blade measurements was to transfer the strain signal into a blade root bending moment. As explained in the paper of Paulsen *et. al.* (Paulsen, Gomiero, Larsen, & Benini, 2018), then static blade pull tests were perform on the turbine and a liniear calibration relation to the bending moment was obtained. This relation was however observed to drift with temperature and time, whereby a calibration procedure was introduced, where the blade picth angle (azimuth angle) was used to correct the blade root strain gauge calibrations at idling conditions of the turbine.

Table 2 List of sensor signals of the V52 research turbine as provide by the Vestas Data Format (VDF) and the additional sensors added by DTU (Reproduced from (Paulsen, Gomiero, Larsen, & Benini, 2018).

Signal	Unit	Type	Notes
Pitch	deg	VDF	Collective pitch angle
Rotor speed	rpm	VDF/DTU	RPM sensor
Azimuth	deg	DTU	Blade A position
El. Power	kW	VDF/DTU	Net available power
MxA	mV/V	DTU	Blade A root flapwise SGs
MyA	mV/V	DTU	Blade A root edgewise SGs
Nacelle wind speed	m/s	VDF	Sonic anemometer
Nacelle Yaw	deg	DTU	Nacelle position

The data from the V52 research turbine of DTU has previous been compared to aero alastic simulations based on a Hawc2 model representation of the V52 research turbine as reported by Rinker *et. al.* (Rinker, Hansen, & Larsen, 2018). Similar comparisons between the blade strain gauge signals and Hawc2 simulations of the the blade root have been performed by Paulsen et. al. (Paulsen, Gomiero, Larsen, & Benini, 2018). Paulsen *et. al.* found resonable good agreement between the measured blade root bending moments as shown in Figure 4 and this is showing that the Hawc2 aeroelastic model of the V52 research wind turbine can be used to determine the bending moment load cycle ranges for fatigue life estimations.

The Hawc2 aeroeleastic model of the V52 research turbine can not be shared un-restricted ourside DTU, since it holds confidential information about the V52 turbine and it was therefore not possible to use the V52 research turbine as a bench mark case for life estimations as original planned in the IEA Task 42. This is illustrating a need for generic aeroelatsic models for life estimations as is shown in chapter 3.

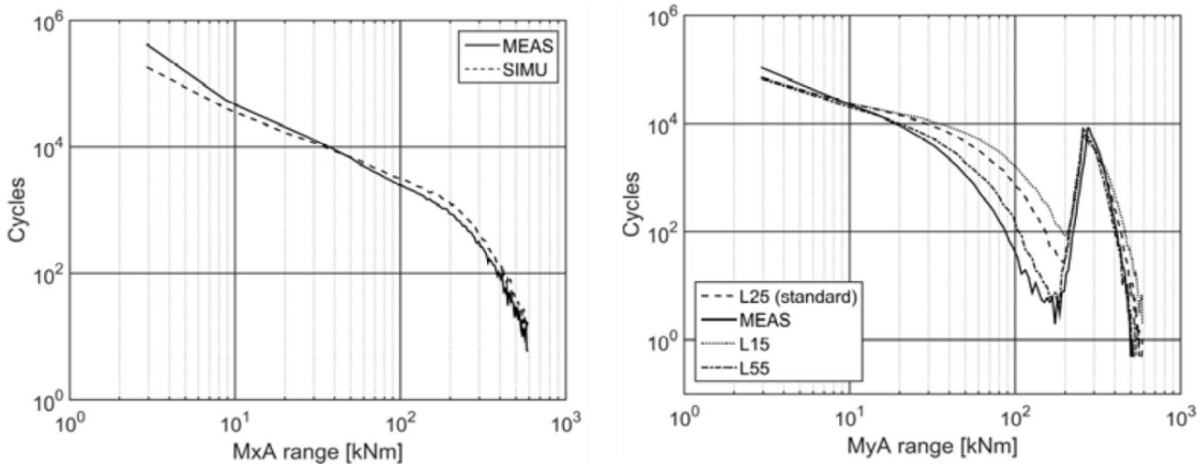

Figure 4 ***Left****: Comparison between measured and simulated blade flapwise bending moments load ranges of the V52 research turbine.* ***Right****: Comparison between measured and simulated blade edgewise bending moments load ranges for different specification of the Mann turbulence model as given by the meteorological length scale L (L = 15 m , 25 m, and 55 m). Reproduced from Paulsen et.al. (Paulsen, Gomiero, Larsen, & Benini, 2018).*

2.2. Alpha Ventus

In addition to the V52 data, in this work, offshore data from a measurement campaign in the German “Alpha Ventus” wind farm are utilised. The raw data are freely available for research purposes after signing an agreement concerning the data usage (https://www.rave-offshore.de/en/data.html). Alpha Ventus consists of twelve 5 MW turbines: six Senvion 5M turbines mounted on jackets and six Adwen 5-116 turbines mounted on tripods (see Figure 5 (left)). The wind farm is located about 45 km north of the German island Borkum (see Figure 5 (right)).

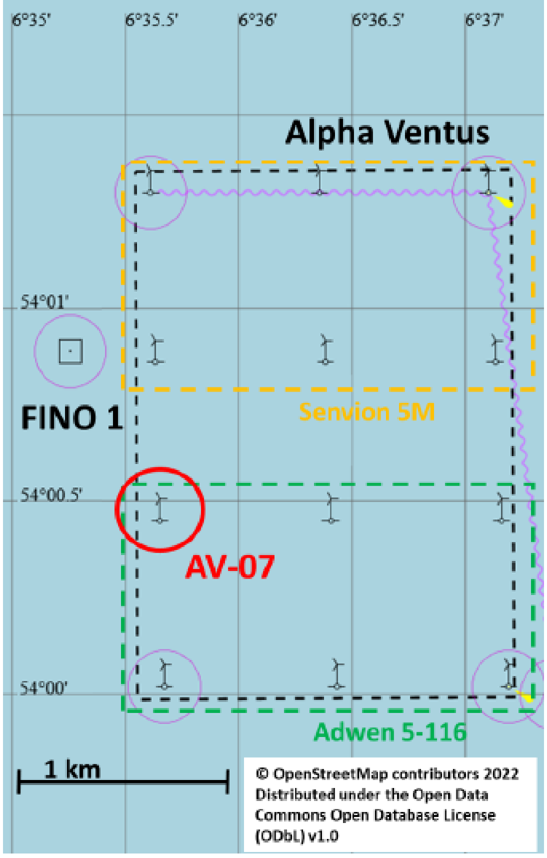

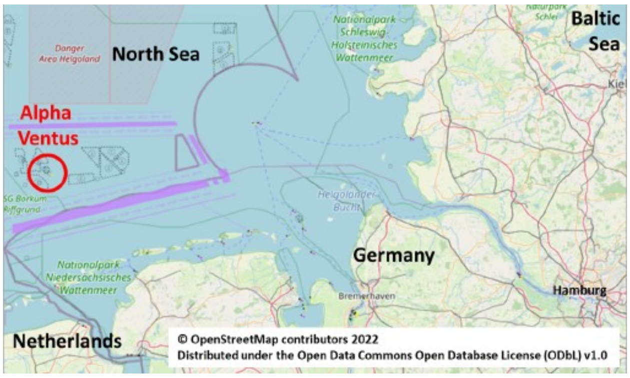

Figure 5: Left, farm layout of Alpha Ventus with considered AV-07 turbine marked according to (Hübler & Rolfes, 2022); right, location of Alpha Ventus and the met mast FINO1 according to (Hübler & Rolfes, 2022)

Table 3: Properties of the investigated AV-07 turbine according to (Hübler & Rolfes, 2022)

Type	Adwen 5-116 turbine
Substructure	Tripod
Rotor diameter	116 m
Hub height	90 m
Water depth	approx. 30 m
Rated power	5 MW
Rotor speed	5.9 – 14.8 rpm
Rated wind speed	12.5 ms^{-1}
Cut-in wind speed	3.5 ms^{-1}
Cut-out wind speed	25 ms^{-1}

The water depth within Alpha Ventus is about 30 m. Alpha Ventus was commissioned in April 2010. The measurement campaign started in 2011. Since then, not only SCADA data are being collected, but environmental conditions, strains, accelerations etc., are measured as well. Further environmental data are available from the metmast FINO1 (https://www.fino1.de/en/). FINO1 is located next to the Alpha Ventus wind farm (cf. Figure 5 (left)). This work focuses on the AV-07 turbine (see Table 3). It is marked in Figure 5 (left). This turbine is equipped with more than 100 sensors on the rotor-nacelle assembly, the tower and the substructure above and below sea level. Data concerning environmental conditions are available as statistical values of ten-minute intervals. Strain data are provided as high resolution (50 Hz) time series for several locations. As an example, this work uses the strain data from one location on the tower, as marked in Figure 6.

Although measurement data are, in general, available for time periods since 2011, for many periods, the data quality is not sufficient for fatigue life predictions. Only the data from three specific years have a sufficient quality to be taken into account: 1st January 2011 to 31st December 2011 and 1st October 2015 to 30th September 2017. Data of the two consecutive years, i.e., 1st October 2015 to 30th September 2017 are used in this work.

For this work, three types of data are required: strain data, data regarding environmental conditions and data concerning operational conditions.

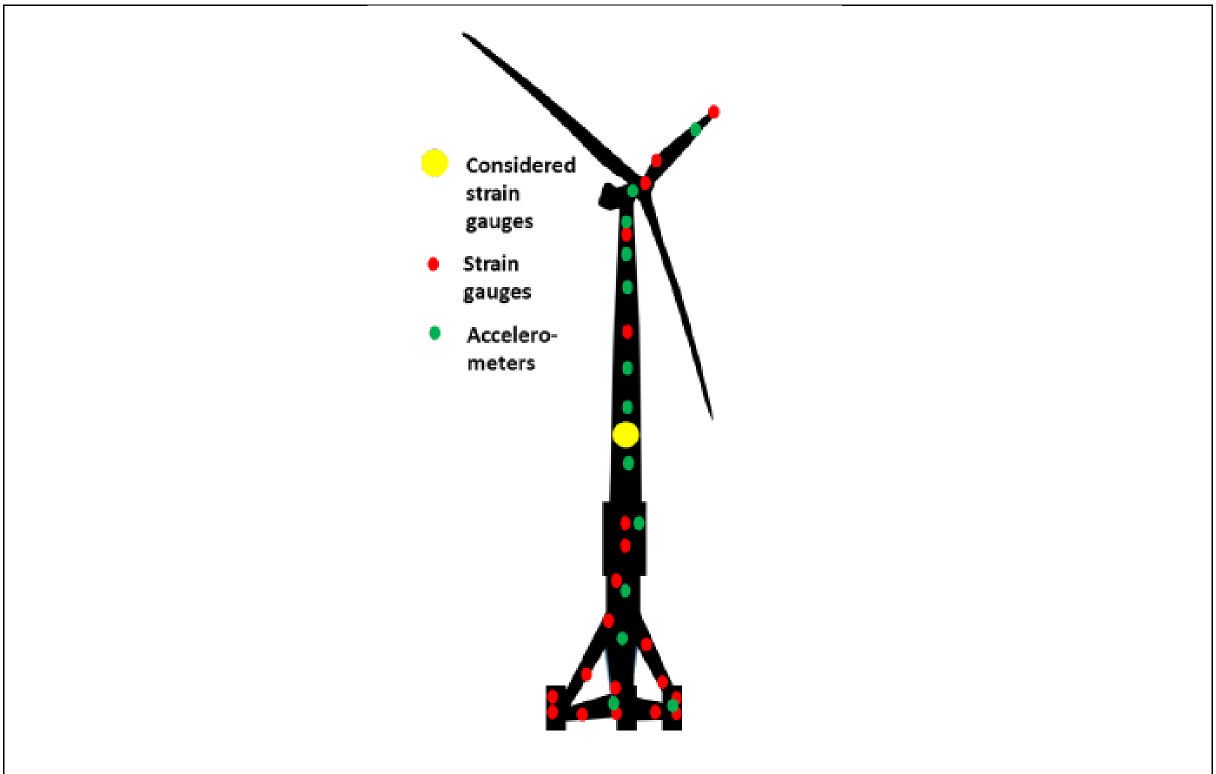

Figure 6: Illustration of the AV-07 turbine (not to scale) and some of the installed sensors according to (Hübler & Rolfes, 2022)

Strains are measured on the tower of the AV-07 turbine. The raw data was post-processed using semi-automatic methods to exclude, for example, erroneous data. See (Hübler & Rolfes,

2022) for more details. Operational conditions are taken from SCADA data from the AV-07 turbine. Environmental conditions are, in most cases, taken from the FINO1 met mast. Only if no data are available from FINO1, the wind conditions included in the SCADA data from the AV-07 turbine are taken into account. Again, more detailed information can be found in (Hübler & Rolfes, 2022). For this work, six environmental conditions, namely wind speed, wind direction, turbulence intensity, significant wave height, wave peak period and wave direction, are considered. In addition, the turbine status – recorded by the SCADA system, e.g., normal operation, start-up, emergency stop, etc. – is taken into account. For all Environmental and Operating Conditions (EOC), only statistical values, e.g., mean values of ten-minute intervals are available.

2.3. German offshore wind farm

The quality of the Alpha Ventus offshore measurement campaign that are freely available was assessed by Wölfel as insufficient for the data-driven life assessment planned. Numerous monitoring systems of Wölfel are installed in offshore wind farms, often fleet-wide. The investigation presented by Wölfel in this report was performed using the Wölfel monitoring system data from a German offshore wind farm. Due to confidentiality, no detailed information can be given regarding the exact number of monitoring systems and sensor layout.

The sensor configuration for 10% of the turbines in the wind farm includes strain gauges and inclination sensors at the tower/TP connection and accelerometers at the tower top. The remaining turbines in the wind farm are also instrumented with an inclination sensor and accelerometer, but have no strain sensors.

3 Lifetime prediction of onshore turbines: A generic approach

Lifetime extension is an elaborate task consisting of a theoretical evaluation of the remaining structural load bearing capacity as well as a practical assessment of the structural health by inspections. The theoretical evaluation seeks to quantify the remaining useful fatigue lifetime of major load bearing components such as the blades and tower. Traditionally, this requires detailed design information about the specific turbine model for the fatigue load simulations, but often this information is either confidential property or simply lost over time. It is therefore critical to develop methods that provide sufficiently accurate fatigue lifetime assessments using whatever models are available at the time of lifetime extension decisions.

Here we show for the Vestas V52 turbine at Risø how the remaining useful fatigue lifetime may be estimated using a publicly avilable generic wind turbine model with similar specifications.

3.1. Load assessment

This section describes the turbines used for load assessment. First the generic turbine is defined, which is selected to resemble the Vestas V52 turbine as close as possible. Then, it is explained how a load model has been trained for the V52 turbine based on the measured data described in section 2.1.

3.1.1. Generic load model

To provide accurate lifetime assessments using a generic turbine model it is essential to chose one that resembles the specific turbine as close as possible. There are multiple publicly available turbines to chose from e.g. the 0.75MW WindPACT turbine (Rinker & Dykes, 2018), the 5MW reference wind turbine by NREL (Jonkman, Butterfield, Musial, & Scott, 2009), or the 10MW reference wind turbine by DTU (Bak, et al., 2013). In this work the 0.75MW WindPACT turbine is chosen due to its similarities to the Vestas V52 as outlined in Table 4.

Table 4: Turbine specifications.

Parameter	Vestas V52	WindPACT 750kW
Rated Power	850kW	750kW
Power regulation	Pitch regulated, Variable speed	Pitch regulated, Variable speed
Orientation	Upwind	Upwind
Number of blades	3	3
Hub height	44 m	60 m
Rotor diameter	52 m	50 m
Rated rotor speed	26 rpm	28.6 rpm
Specific power	400 W/m^2	382 W/m^2
Cut-in windspeed	4 m/s	3 m/s
Cut-out windspeed	25 m/s	25 m/s

To calculate fatigue loads the generic turbine has been simulated in the aero-servo-elastic code FAST (Jonkman J. , 2015) using 100 seeds when generating the input turbulent wind fields. Subsequently, two main load bearing components have been chosen for this study as outlined in Table 5. The fatigue strength of each component is modelled by typical Wöhler exponents (m) used for welded steel details ($m = 4$) and blade composite materials ($m = 10$).

Table 5: Wind turbine components.

Component	Description	Notation	Type	Wöhler exponent
Blades	Blade root flap-wise bending	RootMyb1	DEL	10
Tower	Tower bottom fore-aft bending	TwrBsMyt	DEL	4

3.1.2. Specific load model

To estimate loads on the Vestas V52 turbine a Gaussian process regression (GPR) model was trained using the concurrent wind and load measurements described in section 2.1. Note that only non-waked wind directions were considered for this study to avoid introducing the relatively large uncertainties connected to current engineering wake models.

The data used to train the surrogate model for the tower bottom fore-aft fatigue load is shown in Figure 7 (left). To reduce the amount of input data used for model training (and to reduce the apparent noise) all data has been condensed into 600 points using a k-means clustering technique as shown in Figure 7 (right). Note that this process of associating multiple data points to the same cluster (i.e. wind climate) closely resembles how multiple seeds are considered when doing aero-elastic simulations in order to reduce the effect of random wind field realizations.

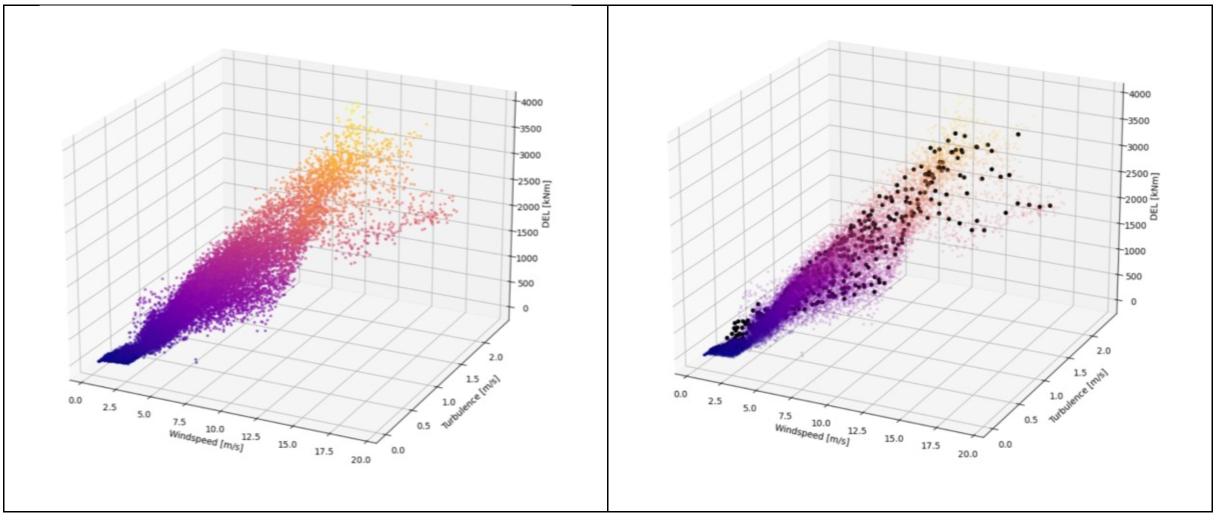

Figure 7: Left, Concurrent measurements of the wind climate and resulting tower fore-aft fatigue loads used for surrogate model training. Right, Data clustering.

The GPR model accuracy has been evaluated by splitting the 600 clusters of data into a traning set and a validation set consisting of 400 and 200 data points, respectively. The two sets are shown in Figure 8 left. In Figure 8 right the model accuracy is illustrated. Notice that the largest errors are gathered at low fatigue load values which makes them insignificant.

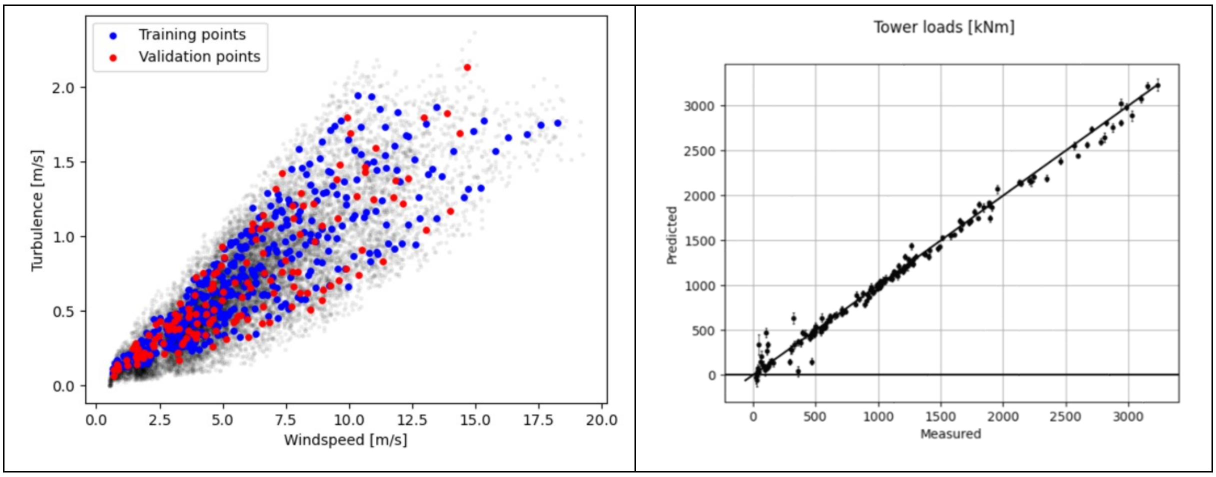

Figure 8: Left, Data clusters shown in 2D split into a training and a validation set. Right, GRP model accuracy for the Vestas V52 turbine tower fore-aft bending moment.

To illustrate the similarity between the Vestas V52 turbine model and the chosen generic 0.75MW WindPACT model their tower load response is compared in Figure 9.

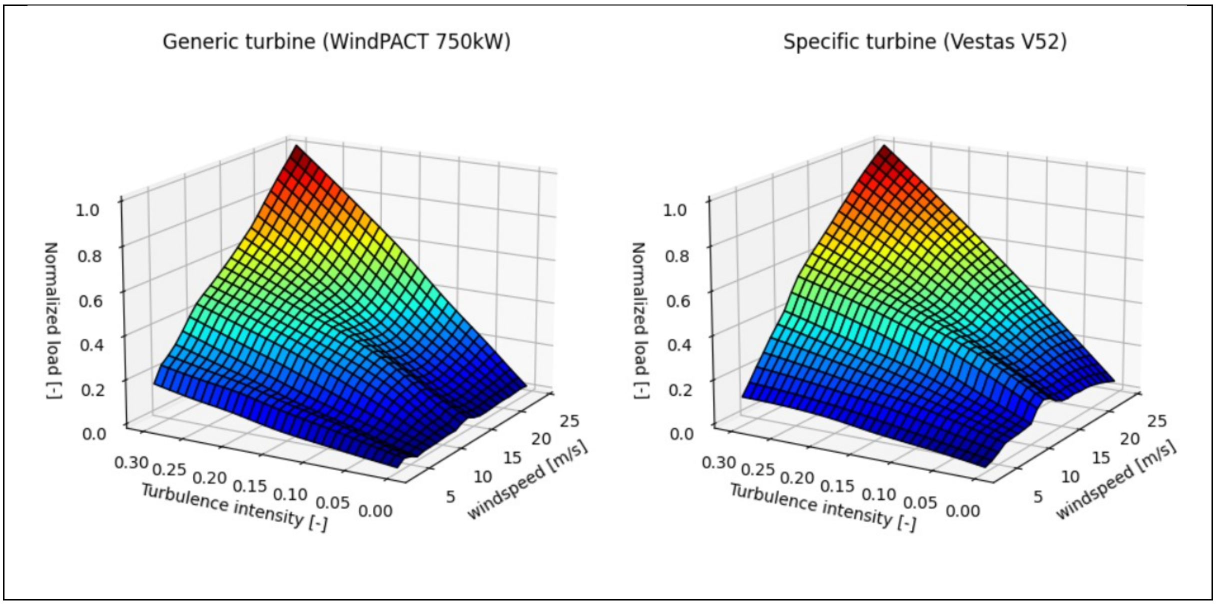

Figure 9: Comparison of tower fore-aft fatigue load response between the generic 0.75MW WindPACT turbine and the specific Vestas V52 turbine.

3.2. Case study: V52 at Risø

Site-specific fatigue loads are calculated in accordance with the IEC 61400-1 design standard (IEC, 2019) design load case 1.2 (normal operation). The site wind climate is estimated based on the same data used to train the specific load model (before clustering), hence it relies on the ambient wake-free wind directions only.

The design class of the Vestas V52 is assumed to be 3C as defined in the IEC standard (IEC, 2019). This is somewhat lower than the actual design class of the turbine, but due to the benign wind climate at Risø in the measured period of time fo 2018 it results in unrealistically high lifetime values if a larger turbine class is assumed.

With the site-specific and design wind climate in place the associated loads were calculated using both turbine models. These loads are then compared and the useful fatigue lifetime is estimated based on their ratio. This procedure is outlined for the tower fore-aft fatigue loads in Figure 10 where a design lifetime of 20 years is assumed.

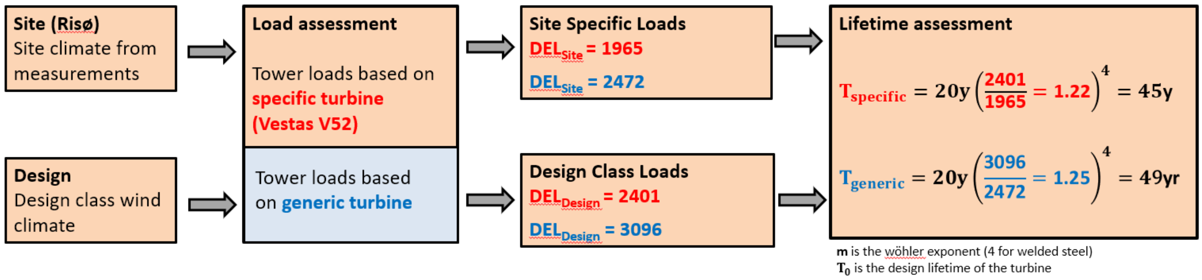

Figure 10 Lifetime assessment of the wind turbine tower.

As shown there is only a very slight difference in the load ratio (1.22 vs 1.25), which translated into ~10% deviation of the lifetime. It is also noticable that the absolute loads on the generic turbine are much higher than on the Vestas V52. This is explained by the difference in tower height (see Table 4), but due to the relative nature of the analysis this apparently large source of error is almost completely cancelled out.

Similar to the tower, the load index and useful fatigue life of the turbine blades was also estimated. The results are summarized in Table 6 and Table 7.

Table 6: Turbine load ratio.

Component	Vestas V52	WindPACT 750kW	Difference
Tower fore-aft	1.22	1.25	2.5%
Blade root flap	1.17	1.20	3.0%

Table 7: Turbine lifetime estimation.

Component	Vestas V52	WindPACT 750kW	Difference
Tower fore-aft	45 years	49 years	9%
Blade root flap	96 years	129 years	25%

Apparently, the error on the blade root flapwise lifetime estimation is quite large, but the magnitude of the error has to be percieved relative to the Wöhler exponent (m=10 for the blades). Basically, the error on the load ratio estimations are amplified by the Wöhler exponent, hence, an important result is that the error on the load ratios are almost identical for the tower and the blades.

3.3. Conclusion

A highly accurate surrogate model was used to predict fatigue loads during normal operation on the V52 turbine located at Risø, Denmark. By comparing site-specific and design loads the theoretical fatigue lifetime of turbine tower and blades were estimated to be 45 and 96 years, respectively.

By recalculating tower and blade loads using the same wind climate input, but this time based on the 0.75MW WindPACT turbine model together with aero-elastic simulation in FAST, comparable lifetimes were obtained. The resulting error on load ratio estimates between the generic model approach and the real Vestas V52 was within ~3%. In terms of lifetime assessment this translates into an accuracy of 10% for the tower and 25% for the blades. The reduced accuracy of the blades can be explained directly by the Wöhler exponent associated to typical blade composite materials which is much higher compared to that of welded steel details in the tower bottom section.

The presented method provides a basis for improved decision support for wind turbine owners when their assets approach their design lifetime and critical investment decisions about possible future operation must be made. At that point it may be difficult, if not impossible, to obtain the full structural information required for aero-elastic simulation. In most cases there is also no data available which contain full information of the turbine loads; hence, an approach is required which does not rely heavily on the specific turbine itself. The results provided here strongly suggests that generic turbines can provide lifetime estimates that are sufficiently accurate for initial decision making before investing further into expensive and time-consuming physical inspections.

Overall, the presented method may provide a more efficient use of our wind resources and at the same time prevent that wind turbines are recycled even though their structural integrity is still intact.

4 Probabilistic temporal extrapolation

In Section 3, an approach making use of public turbine simulation models was presented. This approach has the advantage that neither the turbine model, which as been used during the design phase, is required nor strain measurements at the real turbine. However, if strain data are available, alternative approaches, which make use of the additional information within the strain data, are possible. Such a strain measurement-based approach is presented in this section.

For strain measurement-based approaches, the main challenge is that strain data are limited. This means that measurements are only available for a limited period and only at some specific hot-spot locations. Hence, spatial and temporal extrapolations are required. Available procedures are not yet standardised and in most cases not validated. This section focuses on extrapolations in time. Several methods for the extrapolation of fatigue damage are assessed. The methods are intended to extrapolate fatigue damage calculated for a limited time period using strain measurement data to a longer time period or another time period, where no such data are available. This could be, for example, a future period, a period prior to the installation of strain gauges or a period after some sensors have failed. The methods are validated using two years of strain measurement data from the German offshore wind farm Alpha Ventus (see Section 2.2). The performance and user-friendliness of the various methods are compared. It is shown that fatigue damage can be predicted accurately and reliably for periods where no strain data are available. Best results are achieved if wind speed correlations are taken into account by applying a binning approach.

4.1. Method

The general idea of all approaches in this section is the use of correlations between short-term damage and Environmental and Operating Conditions (EOCs). Such a correlation is shown in Figure 11. For a comprehensive description of short-term damage, the reader is referred to (Hübler & Rolfes, 2022). In a nutshell, a short-term damage value (D_j) is the fatigue damage that is calculated for a ten-minute period when assuming linear damage accumulation.

If strain data were available for the entire lifetime of the wind turbine, it would be possible to determine its fatigue lifetime (D_{total}) by using all short-term damage values in the following way:

$$D_{total} = \sum_{j=1}^{N_{LT}} D_j$$

where N_{LT} is the number of (short-term) intervals in the entire lifetime, e.g., $N_{LT} = 6 \times 24 \times 365.25 \times 20$ for a lifetime of 20 years.

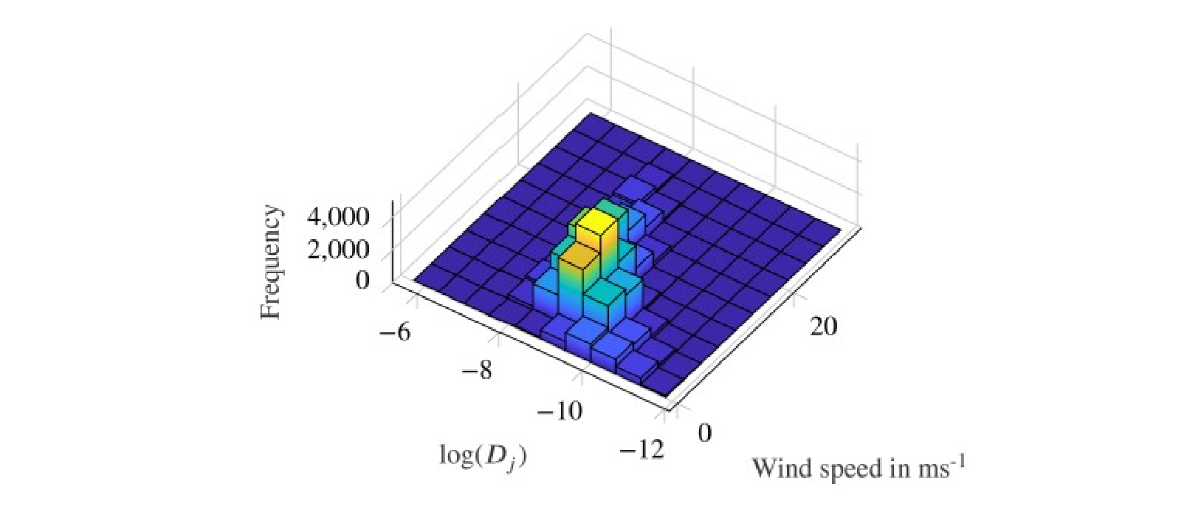

Figure 11: Correlation of wind speeds and logarithmised short-term damage values (D_j). Histogram based on all 10 min intervals in 2016; according to (Hübler & Rolfes, 2022).

However, normally, strain data are not available for the entire lifetime. Therefore, some kind of extrapolation procedure in time is necessary. In the following, three different approaches are presented: a simple linear extrapolation, an extrapolation based on bins of EOCs and an extrapolation based on machine-learning techniques.

4.1.1. Simple extrapolation

The simplest extrapolation approach is a linear extrapolation. It assumes that fatigue damage only depends on the elapsed time (Loraux & Brühwiler, 2016). This means that the fatigue damage sustained in any predicted period can be calculated as follows:

$$D_{pred} \approx \frac{N_n}{N_m} \sum_{j=1}^{N_m} D_j$$

where N_m and N_n are the number of (short-term) intervals in the measurement and the predicted period respectively. If the predicted period is the entire lifetime, $D_{pred} = D_{total}$.

For very long measurement periods ($N_m \approx N_{LT}$), this approach yields accurate results. However, if the measurement period is less than one year, seasonal effects are neglected.

4.1.2. Extrapolation based on bins of EOCs

A more advanced approach, which makes use of the correlation between fatigue damage and EOCs (cf. Figure 11), is a so-called binning approach ((Marsh, 2016); (Hübler, Weijtjens, Rolfes, & Devriendt, 2018)). This binning approach is still very simple to apply, and therefore, quite user-friendly. The binning approach is based on the idea that most variations in fatigue damage are due to changing environmental conditions. Hence, it is not necessary to know fatigue damage for the entire lifetime. Having determined the correlation between EOCs and fatigue damage, it is sufficient to know the EOCs for the entire lifetime. Since many EOCs are part of the SCADA data, EOCs are frequently known for the entire lifetime. Hence, the only challenge is determining the correlation between fatigue damage and EOCs. For the binning approach, the (short-term) damage values are clustered according to the EOCs. For each cluster or bin, the mean damage is determined using the available measured strain data. Subsequently, the damage sustained in the predicted period is:

$$D_{pred} \approx N_n \sum_{i_1=1}^{M_1} \dots \sum_{i_d=1}^{M_d} (Pr_{pred,i_1,\dots,i_d} \, \overline{D}_{i_1,\dots,i_d})$$

where d is the binning dimension – i.e., the number of EOCs considered, M_1 to M_d are the number of bins for the corresponding EOC and $Pr_{pred,i_1,\dots,i_d}$ and $\overline{D}_{i_1,\dots,i_d}$ are the occurrence probability of and the mean damage in bin $i_1, \dots, i_d$ respectively. Mean damage within the bins can be determined using a limited amount of strain data, e.g., one year (measurement period). To determine the bin probabilities, only data concerning the EOCs are required. Hence, bin probabilities are determined using data of the predicted period. If the predicted period is the entire lifetime, it follows that $D_{pred} = D_{total}$ and $Pr_{pred,i_1,\dots,i_d} = \ Pr_{LT,i_1,\dots,i_d}$.

In contrast to the previously presented simple extrapolation, seasonal effects and long-term changes due to changing EOCs are taken into account by the bin probabilities. The main challenge of the binning approach is to apply expedient binning dimensions and bin numbers. For more details regarding the binning approach, the reader is referred to (Hübler & Rolfes, 2022).

4.1.3. Extrapolation based on a functional relationship

The correlation between short-term damage and EOCs can also be expressed more generally as a functional relationship, i.e., $D_j = f(\boldsymbol{x}_j) + \epsilon$, where $\boldsymbol{x}_j$ is the vector of all EOCs considered in the analysed interval j and ϵ is an error term, which cannot be explained by changes in the EOCs considered. Such a functional relationship can be approximated using various statistical and/or machine-learning techniques, e.g., multiple regression, Gaussian process regression (GPR), artificial neural networks (ANN) etc. To determine the functional relationship, training data are required to train the relation between inputs, i.e., EOCs, and outputs, i.e., fatigue damage values. Similar to the binning approach, it is not necessary that strain data are available for the predicted period or the entire lifetime. The strain and EOC data from the measurement period, e.g., one year, are used as training data. Subsequently, fatigue damage for other time periods can be predicted using EOC data only. EOC data are normally available for the entire lifetime.

$$D_{total} \approx \sum_{k=1}^{N_{LT}} f(\boldsymbol{x}_k)$$

The accuracy of the prediction also depends on the EOCs considered. In this work, GPR and ANN are investigated. Both methods are very powerful machine-learning techniques. On the downside, they are less user-friendly compared to the binning approach. At least some expert knowledge is required to achieve accurate predictions.

All configurations for ANN and GPR used in this work are summarized in (Hübler & Rolfes, 2022).

4.2. Results and validation

As discussed in the previous subsection, for the binning approach as well as for machine learning approaches, the number and the kind of EOCs that are taken into account are essential. Therefore, for both approaches, the optimal EOCs are determined using measurement data of the Alpha Ventus wind farm (see Section 2.2).

4.2.1. Parameter selection

The choice of optimal EOCs (number and type) might be influenced by the period investigated. Hence, optimal EOCs are determined using several periods. However, only three years of data are available and only two of these years are consecutive years, for which long-term effects can be excluded. Hence, within the two consecutive years, a one-year period is shifted, e.g., October 2015 to September 2016 is extrapolated to October 2016 to September 2017, November 2015 to October 2016 is extrapolated to October 2015 and November 2016 to September 2017, etc. Using these shifted periods, 13 "different" periods are available, which yields at least some statistical significance for the determined parameters.

4.2.2. Parameter selection (simple extrapolation)

For the simple extrapolation, no parameters have to be chosen. First results for the simple extrapolation are presented in Figure 12. For all 13 one-year periods, the unsigned percentage errors (PE) of the predicted yearly damage are shown:

$$PE = \left|\frac{D_{real} - D_{pred}}{D_{real}}\right|$$

Moreover, a box plot shows some summary statistics: the median (red centre line), the 25th and 75th percentile (box), the minimum and maximum values (excluding any outliers) and possible outliers of 13 "different" one-year measurement periods. Hence, the box plots visualise the variation in the accuracy of the predictions depending on the period considered. All box plots in the following subsections show the same summary statistics.

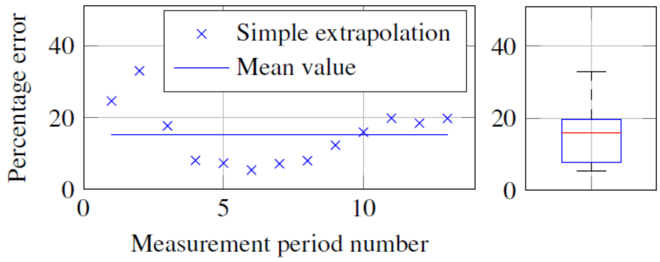

Figure 12: Percentage errors of predicted yearly damage values using a simple extrapolation method compared to real yearly damage values. Prediction from one year to a second year for 13 "different" years. Box plot shows summary statistics. Figure taken from (Hübler & Rolfes, 2022).

Clearly, the prediction does not yield precise results. Nonetheless, it is remarkable that even such a simple extrapolation leads to results with errors of less than 35 %.

4.2.3. Parameter selection (EOC bins)

For the extrapolation based on bins of EOCs, the number and type of EOCs to be taken into account and the bin size must be selected. In contrast to previous work ((Loraux & Brühwiler, 2016); (Hübler, Weijtjens, Rolfes, & Devriendt, 2018)), who focused on one to three different wind parameters, in this work, six different environmental conditions (wind speed and direction, turbulence intensity and wave height, period and direction) are analysed in a systematic manner. Bin sizes are chosen in such a way that the overall range of each environmental condition is discretised into about 3 to 120 bins depending on the environmental condition. For example, bins of 0.25 to 6 m/s are used for the wind speed.

Some example results for the binning approach are presented in Figure 13. A detailed discussion of the results is given in (Hübler & Rolfes, 2022). As a summary: the choice of the bin dimension and size is of minor importance as long as empty bins do not occur at all or only in some rare cases. For most applications, simple wind speed bins with a size of 2 to 3 m/s are adequate.

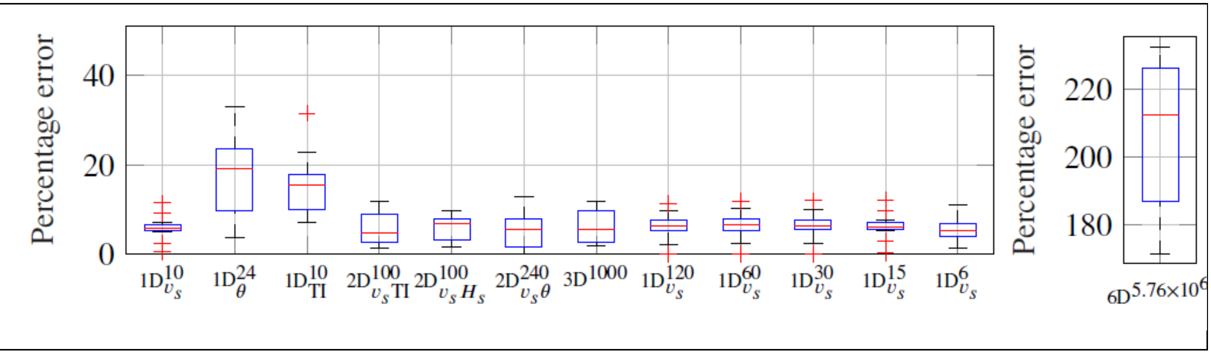

Figure 13: Percentage errors of predicted yearly damage values using a binning method compared to real yearly damage values. Comparison of various bin types and sizes (n is the overall number of bins): wind speed (v_s), wind direction (θ) and turbulence intensity (TI) only ($1D^n_x$); combinations of two environmental conditions out of wave height (H_s), v_s, θ and TI ($2D^n_{xy}$); v_s,, TI and H_s (3D); all six environmental conditions (6D). Please note: for the sake of clarity, the vertical axis is scaled differently for 6D. Figure taken from (Hübler & Rolfes, 2022)*.*

4.2.4. Parameter selection (Functional relationship)

For the extrapolation based on a functional relationship, only the number and type of EOCs to be taken into account are relevant. The same six environmental conditions as before are considered. Some example results for the functional relationship are presented in Figure 14. Again, the detailed performance depends significantly on the measurement period (cf. scatter shown by the box plots).

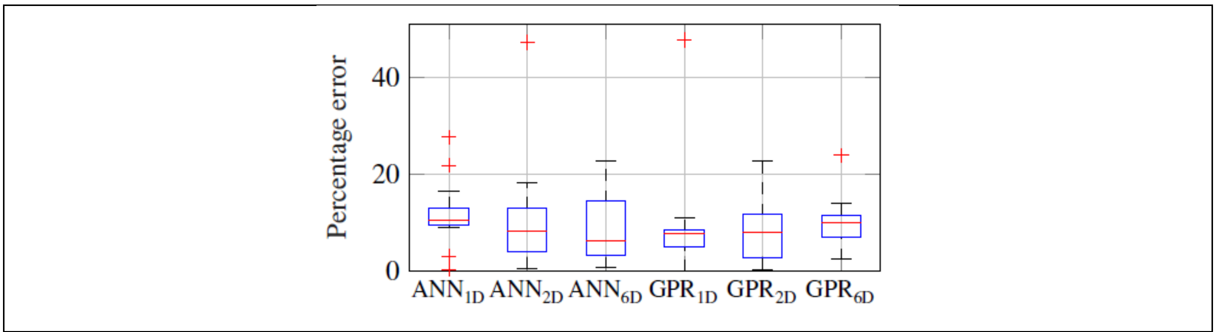

Figure 14: Percentage errors of predicted yearly damage values using a functional relationship compared to real yearly damage values. Comparison of GPR and ANN and different EOCs: v_s (1D); v_s and TI (2D); all environmental conditions (6D). Figure taken from (Hübler & Rolfes, 2022).

A slight improvement in the accuracy might be achieved for ANN if additional environmental conditions are taken into account. However, this improvement is not significant. At least for wave conditions, it definitely does not justify the effort needed to measure them.

Therefore, in the following, only results using a single environmental condition, i.e., the wind speed, are shown.

4.2.5. Operational conditions

In addition to the environmental conditions discussed in the previous subsections, it is also possible to consider operational conditions. However, as shown by (Hübler & Rolfes, 2022), the use of operational conditions for the temporal extrapolation of fatigue loads does not improve the accuracy significantly. Therefore, in the following, operational conditions are not considered.

4.2.6. Validation and comparison

Knowing the optimal EOCs for all approaches, the approaches can be validated using measurement data and compared to each other. As stated in Section 4.2.5, no clustering according to operational conditions is applied. For the binning approach, only wind speed bins with a bin size of 3 m/s are used. Similarly, only wind speed correlations are taken into account for ANN and GPR. These choices are in accordance with the findings of Section 4.2.3 und 4.2.4.

In Figure 15, the percentage errors of predicted yearly damage values of all approaches for all 13 years are shown.

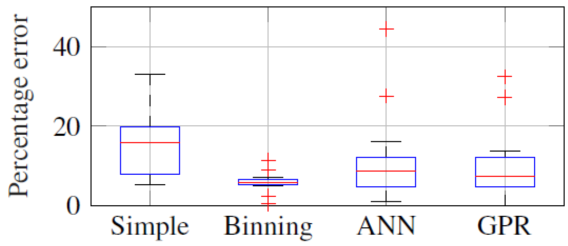

Figure 15: Percentage errors of predicted yearly damage values using all extrapolation methods compared to real yearly damage values. Predictions from one year to a second year for 13 "different" years). Figure taken from (Hübler & Rolfes, 2022).

It becomes apparent that the binning approach reduces the percentage error on average by about 60 % compared to the simple extrapolation (cf. red centre lines of the box plots). Moreover, the binning approach outperforms ANN and GPR. However, two facts about ANN and GPR should be mentioned. First, the initial weights used by ANN and the subsets used by GPR are chosen randomly. Hence, the performance of both is not deterministic, but features some kind of model uncertainty. In order to assess the performance of ANN and GPR with some statistical evidence, several, i.e., 100, ANNs and GPR models are trained using the same training data but varying initial weights or subsets. The extrapolation results of the 100 trained models are averaged to rule out the model uncertainty. This yields mean percentage errors of the predicted yearly damage values of all 100 runs and 13 years of 10.3 % and 8.9 %, for each method respectively. Hence, on average, both are outperformed by the binning approach, which yields a mean percentage error of all 13 years of 5.9 % (cf. red centre line of the box plot in Figure 15). Second, it might be possible to improve the accuracy of the machine-learning approaches by exploiting their full potential, e.g., by using more hidden layers for ANN etc. However, a comprehensive analysis of the machine-learning approaches is beyond the scope of this work, as a user-friendly extrapolation approach is being sought. Moreover, (d N Santos, Noppe, Weijtjens, & Devriendt, 2022), who analysed ANN in more detail in the context of fleet-wide extrapolations, also found out that predictions – using ten-minute SCADA data only – lead to percentage errors of up to 10 % in damage-equivalent loads. They showed that ANN is suitable for highly accurate predictions if more or better measurement data (e.g., one-second SCADA data) are available, but not for user-friendly predictions based on ten-minute SCADA data, which are the focus of this work.

To summarise, the simple extrapolation works relatively well. However, if ten-minute SCADA data are available, the binning approach clearly outperforms the simple extrapolation with respect to accuracy. The computing time and the user-friendliness of the binning approach are comparable with the simple extrapolation. For expert users and high quality data, ANN and GPR might be alternatives. For the current application, they are less accurate. Moreover, the machine-learning approaches, especially GPR, have significantly higher computing times.

4.3. Discussion

The work in Section 4 addresses extrapolations of strain measurement-based fatigue damage calculations to other time periods. Several approaches making use of the correlation of EOCs (ten-minute mean values) and short-term fatigue damage values are enhanced, assessed and validated using real offshore measurement data. The approaches are a simple extrapolation, a binning approach and two machine-learning approaches. To summarise the most important results:

- User-friendly binning approaches yield accurate results.
- More complex machine-learning approaches do not yield better results for the given data type, i.e., ten-minute EOC data.
- It is sufficient to consider wind speed correlations only. Other environmental conditions do not need to be taken into account for locations at the tower.

Therefore, user-friendly binning approaches are a suitable alternative or addition to simulation-based lifetime extensions (e.g., Section 3), even if only limited strain data are available. However, some limitations of the approaches in this section should be discussed.

First, spatial extrapolations, i.e., extrapolations to other locations on the same turbine and/or to other turbines in the same wind farm, are not addressed. For spatial extrapolations, the reader is referred to current research, e.g., (Noppe, Hübler, Devriendt, & Weijtjens, 2020) or (Ziegler, Cosack, Kolios, & Muskulus, 2019). Second, only ten-minute data are used. This is reasonable, since ten-minute SCADA data are nearly always available. Nonetheless, (d N Santos, Noppe, Weijtjens, & Devriendt, 2022) already showed that additional data, e.g., one-second SCADA data, are valuable for machine-learning approaches. And third, all present analyses are only conducted for one turbine and one location.

5 Indirect lifetime estimation

As part of the German research project "Life Odometer", TU Munich is looking into the question of how the lifetime consumption of a wind turbine can be quantified without having access to high-frequency load measurements over its whole lifespan. For this, the TU Munich has developed a methodology that uses standard SCADA measurements, meteorological reanalysis data and a database of simulated load time series that are then evaluated using common fatigue calculation algorithms. Since the research project started later than Wind Task 42, only preliminary results are available, which can be explored in more depth in an extension of Task 42.

In Figure 16 this process is illustrated. The first step is to reconstruct the ambient conditions prevailing at the specific site using all available data sources, specifically operational data that is available at every turbine and meteorological reanalysis data that is available online. Before using the data, any statistical errors must be corrected. Using analytical wake models, the wind turbine-specific inflow at each turbine can then be estimated, considering wakes from neighboring turbines, heterogeneous inflow due to terrain effects and the atmospheric condition. With the average characteristics of the wind flowing into the respective plant, a turbulent wind time series can be generated with suitable models such as TurbSim. These serve as input for aeroservoelastic simulations, which model the structural response of the turbine and provide load series as output. These load series can then be further processed to obtain fatigue and consumed life estimates. Another important aspect is the evaluation of the uncertainties in the calculated lifetime consumption to consider both the safety requirements for the stability and operational reliability of the wind turbines and their competitive price.

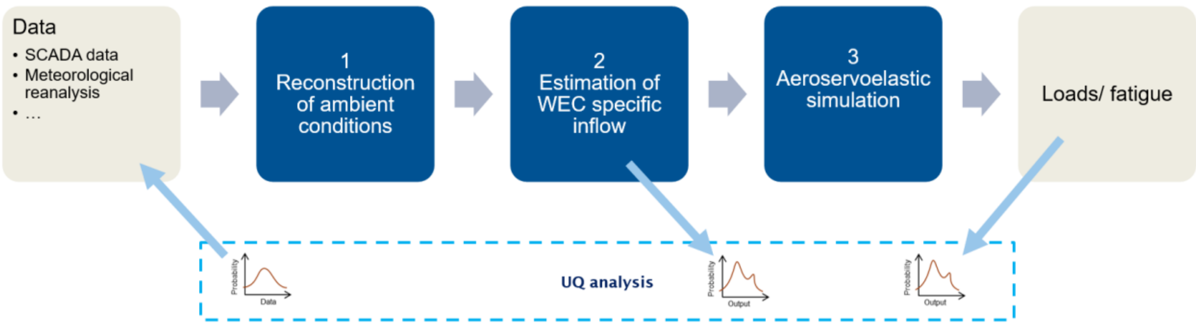

Figure 16: Flowchart of methodology to reconstruct fatigue without load measurements

5.1. Reconstruction of ambient conditions

As the main data source for fatigue reconstruction, 10-minute SCADA data was chosen because of availability and general applicability of the methodology. Due to the location of the anemometer on the nacelle, its measured wind speed is affected by the turbulence created by the rotor. Rotor effective wind speed can be calculated which provides a better estimate of the wind speed (Soltani, et al., 2013). The yaw angle can be used as a wind direction estimator. However, as the yaw angle is often not exactly calibrated to north the bias must be corrected before using it as a wind direction indicator. Furthermore, the turbine can be misaligned. Hence, in order to have a reliable wind direction estimate, the average yaw should be taken of several turbines inside a farm. The TI is defined as the ratio between the standard deviation of the wind speed and the mean wind speed in a 10-minute interval and can be obtained from the SCADA data.

For periods when SCADA data is not available, meteorological reanalysis can be used to supplement the dataset with information on atmospheric conditions. Suitable databases are the ERA5 single level data from ECMWF and the New European Wind Atlas (NEWA) (Jourdier, 2020). As reanalysis data comes at a different temporal and spatial resolution, is only available for certain heights above ground, the data must be processed to have the same characteristics as the SCADA data (see Figure 17).

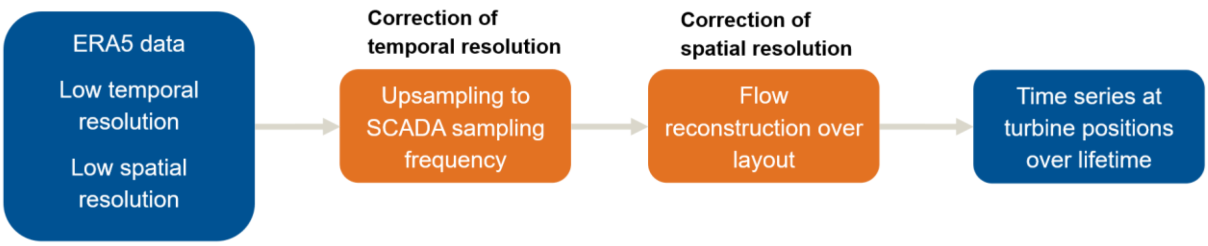

Figure 17: Processing of meteorological reanalysis data

Since the data sampling of the single-level ERA5 dataset is hourly and that of the NEWA dataset is every 30 minutes, the data must be up-sampled to the 10-minute range. This can be done using simple interpolation methods, but the disadvantage of interpolation is that some features of the 10-minute SCADA data do not match. Because of the sampling frequency, the variations in wind speed that are included in the SCADA measurements are not included in the interpolated ERA5 or NEWA data (see Figure 18).

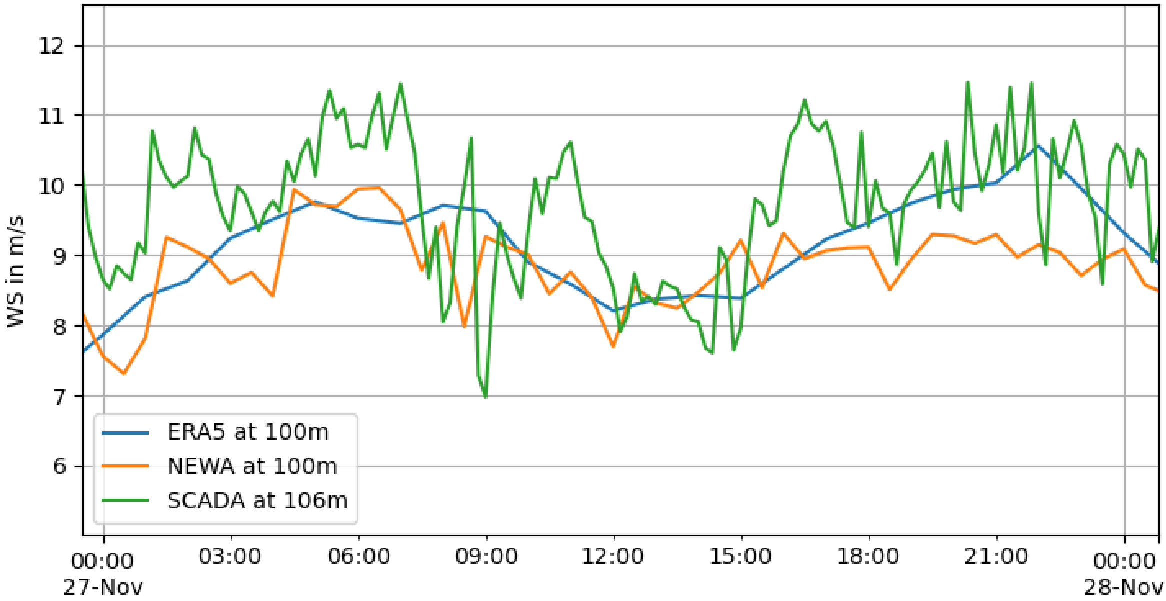

Figure 18: One day of wind speed measurements at offshore wind farm Westermost Rough

The smoothing of the signal compared to the SCADA data ultimately leads to an underestimation of fatigue when ERA5 data are used instead of SCADA data. On the one hand, this is because damage does not increase linearly with wind speed, so fluctuations above the mean have a different effect on damage than fluctuations below the mean. On the other hand, smoothing the signal reduces the amplitude of the low-frequency transition load cycles in the 10-minute range.

For turbines with hub heights that differ from the ERA5 or NEWA heights, the wind speeds must be calculated to account for a vertical wind profile. In addition, statistical biases between data sets must be corrected. A black-box approach that corrects all statistical errors in one shot and also has the potential to model the fluctuations is the use of artificial neural networks. In particular, recurrent neural networks such as LSTMs appear promising for this task. Further research will clarify the applicability and generality of these methods.

Even though the ambient conditions are known, the wind conditions can still significantly vary at the turbine due to local flow effects due to the terrain, neighboring turbines and other obstacles. Therefore, TU Munich developed a method that identifies local flow effects from operational data (Braunbehrens, Vad, & Bottasso, 2022). This method yields spatial correction terms for different ambient conditions.

5.2. Determination of the WEC-specific inflow

Using Floris (NREL, 2021), the local steady state inflow into the rotor plane can be calculated for a specific ambient condition. Figure 19 illustrates a simulated flow field with a heterogeneous flow for a wind direction of 290° at a small wind farm in North Germany. Note that the turbines have varying hub heights, but the plane is at 57m height. Turbine A4 is affected by several turbines and experiences a complex inflow including several wakes and vertical wind shear (Figure 19). This creates a complex inflow into the rotor plane with a spatial variation of the wind speed and the TI (Figure 20).

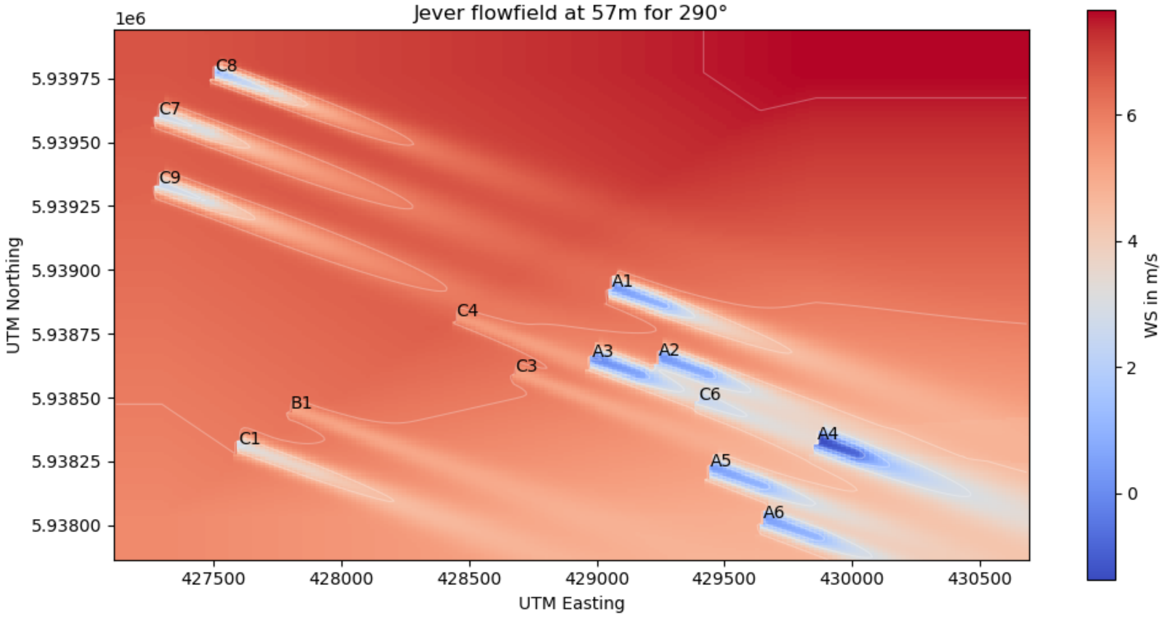

Figure 19: Horizontal flow field at 57m in wind farm Jever

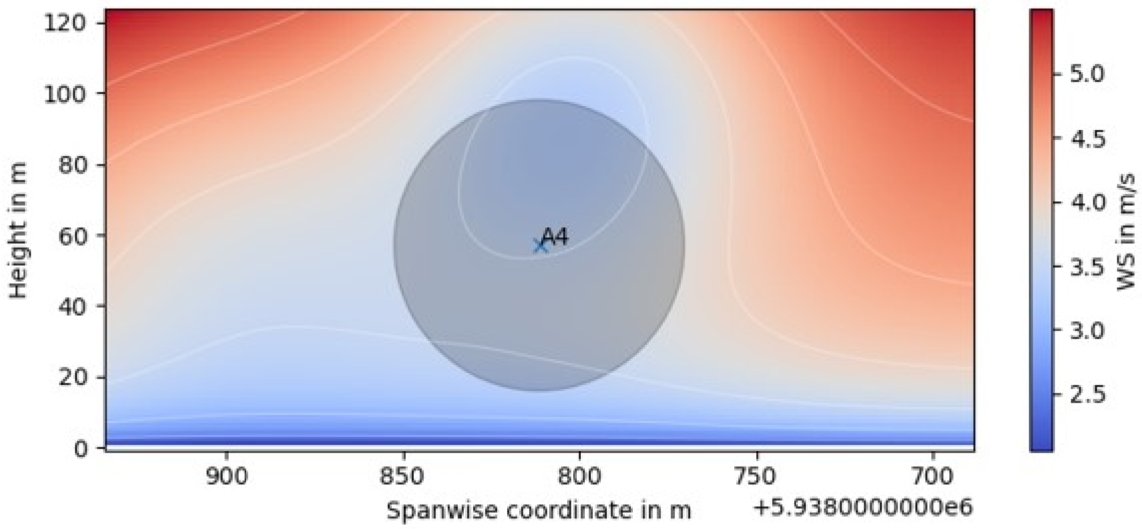

Figure 20: Inflow into rotor plane of turbine A4

From Floris, heterogenous inflow velocities are extracted from grid points just ahead of each wind turbine. Turbulence intensity with wake added turbulence can be obtained at hub height and at all grid points. These average quantities are used to generate, first, a homogeneous turbulence field based on wind speed and TI at hub height obtained from Floris, and then, the heterogenous wind speeds are superimposed on the turbulent time series as speed up factors. Influence of wake meandering will be studied by comparing loads with and without it, while determining WEC (wind energy converter) specific inflow. A comparison is also planned to study the influence of TI distribution on rotor plane and single TI at hub height value on loads from wake affected turbines.

The toolchain will also be compared with existing methods such as FAST.Farm (Jonkman & Shaler, 2021) and Upwind turbine wake in BLADED to understand if a trade-off can be obtained between accuracy and computation effort.

5.3. Aeroelastic simulation and fatigue calculation

The heterogeneous turbulent time series is given as input for aero-servo-elastic simulations. Based on the reconstruction of ambient wind conditions as 10 min values, a comprehensive loads lookup table is created comprising various inflow and operating conditions experienced by all wind turbines in the farm. These inflow and operating conditions are listed in Table 8:

Table 8: Inflow and operating conditions considered in aeroelastic simulations

Inflow conditions	Operating conditions
Wind speed	Normal operation
Wind direction	Derated operation (Sector/Noise mode)
Turbulence intensity	Idling (controlled)
Atmospheric stability	Start-up
Vertical shear	Normal stop

Multiple seeds are run to reduce the uncertainty of turbulence generation. Load series are obtained on critical fatigue components such as blade roots and tower base. Rainflow counting is carried out to identify the load reversals and Palmgren-Miner linear damage rule is used to compute the fatigue accumulated on each component. Additionally, Damage Equivalent Load (DEL) values are evaluated for each seed and eventually a Lifetime DEL can be calculated based on the probability distribution of the different inflow and operating conditions experienced by the turbine. The entire tool chain of determining WEC specific inflow and subsequent fatigue computation from aero-servo-elastic simulations is shown in Figure 21.

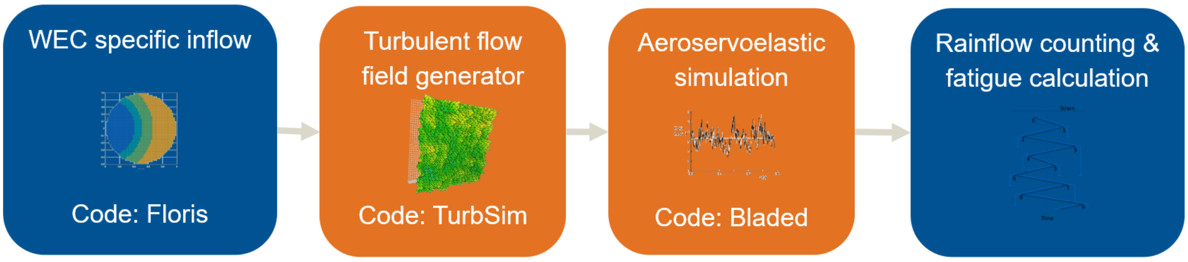

Figure 21: Flow estimator & Fatigue computation tool chain

5.4. **Summary**

A generic approach to reconstruct the accumulated fatigue of a turbine over its lifetime was presented. This can be done without additional measurement equipment on the turbine. Nevertheless, the methodology must be tested and validated against high frequency measurements of blade and tower loads. This is ongoing work and will be presented in future publications or in a possible extension of Wind Task 42.

6 Load reconstruction for fleet monitoring and lifetime extension

This chapter presents the investigations of Wölfel with respect to the estimation of loads at critical sections of offshore wind turbine support structures aiming at the monitoring of the entire wind farms and the extraction of information regarding service lifetime extension. The results of this investigation are presented in (Tsiapoki, Colomer Segura, & Ebert, 2022)[1].

The key performance indicators and results that should be generated by SHM systems for offshore wind turbine generators (WTGs) are indirectly defined by the design verifications that need to be performed regarding the ultimate limit states, serviceability and fatigue (VDI, 2020). Fatigue loads at representative areas of the WTGs are, in addition to vibration amplitudes, modal parameters and measured inclinations, essential features for the assessment of the structural integrity of the tower and foundation. While damage due to extreme load cases is usually unpredictable, damage due to fatigue loading can be prognosed. In order to achieve that, a suitable monitoring concept of the occurring fatigue loads and an established damage accumulation model are required. From the wind farm operator point of view, the knowledge about the applied fatigue loads is of great importance, as it can significantly support data-based decisions for the lifetime extension of offshore wind farms, which can result in significant reductions of electricity production costs. Moreover, the early detection of excessive fatigue damage accumulation can prevent high maintenance and repair costs and, with timely countermeasures, help extend the remaining service life.

A Structural Health Monitoring (SHM) system for offshore wind turbines should be capable of providing information regarding the structural integrity, the acting fatigue loads and the experienced cumulative fatigue damage. A prerequisite for achieving the latter goals is the reliable determination of the internal loads and damage equivalent loads at representative areas of the structures, such as the tower-transition piece or transition piece-monopile connection. These features can then be exploited to assess the remaining fatigue life.

The reliability of the information extracted from the monitoring system regarding the loads actually experienced by the structure and the actually available fatigue damage, increases with the duration and the extent of the available measurements. In offshore wind farms, specifically, the continuous data acquisition from the commissioning of the wind turbines has become state of the art. In order to assess the fatigue lifetime consumption, the fatigue damage determined from the monitoring data is compared with the fatigue damage assumed in design for a certain time period. This comparison is usually performed at the level of Damage Equivalent Loads (DEL), and more specifically, for the tower/TP interface. The allowable DEL are established

[1] The contribution presented in this chapter is a translation of the publication (Tsiapoki, Colomer Segura, & Ebert, 2022).

during the design process, providing a simple quantification of the load cycles that the support structure can sustain, encapsulating all fatigue details.

If the calculated DEL are smaller than those assumed in design, a service life extension for the considered structural components is possible from a fatigue loading perspective. After only a few months, 'conspicuous' turbines can be identified and measures can be taken to optimize their operation. In this manner, data-driven decisions in operation and asset management can be supported. Furthermore, these valuable results can be considered in the scheduling of recurring inspections, lead to cost reduction of wind farm operation and provide a basis for risk-based inspection.

Often the determination of fatigue life consumption takes place under consideration of linear damage accumulation theory according to the Palmgren-Miner rule. For this purpose, rainflow classification is applied on the measured loads to determine the DEL. A direct measurement of the tower and TP bending moments is possible over the application of several strain gauges (or other strain sensors) around the cross section circumference. This method of direct measurement requires comparatively high installation and maintenance costs and accessibility to the cross section of the structure that is as undisturbed as possible (free of attachments and built-in parts), which is not always given.

Load reconstruction methods, i.e. methods for the indirect determination of loads, have been established as an alternative to direct strain measurement and as a cost-effective solution for the structural monitoring of wind turbines.

In many offshore wind farms, approximately 10 % of the WTGs are equipped with a SHM system, which includes the direct strain measurement at representative elevation levels of the structure, usually the transition between the tower and foundation. The last years there is an increasing trend of equipping the remaining 90 % of the wind farm WTGs with a SHM system which has a reduced number of sensors.

The contribution of Wölfel presents a practical approach for the fleet-wide determination of fatigue loads and the derived lifetime consumption. The approach presented uses dynamic responses recorded at the tower top and bottom and a finite element (FE) model to determine the internal forces and bending moments of the structure. Various prediction models are built by combining different aspects, such as the available measurement positions or assumptions regarding the load model and FE model, and are evaluated in terms of their accuracy. Furthermore, the load reconstruction uncertainties introduced by the data acquisition and the model accuracy are discussed. The presented approach is validated using data acquired in an offshore wind farm. The loads at the tower/TP interface are reconstructed based on the conjunction of the dynamic acceleration responses of the tower top or nacelle and a FE model and validated with the corresponding reference values from directly measured strain data. This direct measurement is available at 10% of the wind farm WTGs. After the validation has been concluded, the load reconstruction is applied to the remaining turbines of the wind farm (about 90 % of the structures), where only acceleration data at the tower top are recorded. This holistic fatigue assessment provides insight into the lifetime consumption of the entire wind farm and also allows the identification of correlations to specific events or environmental and operating conditions.

6.1. Method for the estimation of fatigue loads

There are two approaches regarding the load estimation within a wind farm, depending on the existing instrumentation:

- Few turbines in the farm are instrumented with strain gauges and serve as validation objects for the load reconstruction in the wind farm. In this case, the remaining turbines, that are not instrumented with relatively expensive strain sensors, benefit from the validation at the reference objects. In this manner, the overall uncertainty of the load determination and lifetime estimation can be reduced. This case applies to most offshore wind farms.
- All turbines in the wind farm are only equipped with acceleration or inclination sensors and have no strain gauges. The fatigue load estimation is done exclusively with indirect load reconstruction methods (combination of sensor data and FE model). A validation in the wind farm is then not possible.

The proposed approach for the fatigue load estimation based on the combination of structural responses and a FE model is presented in the following section. Subsequently, the uncertainties present in the load estimation from strain data as well as from load reconstruction are discussed.

6.1.1. Load reconstruction approach

The load reconstruction approach consists of a load model, an FE model and the measured structural responses (Figure 22).

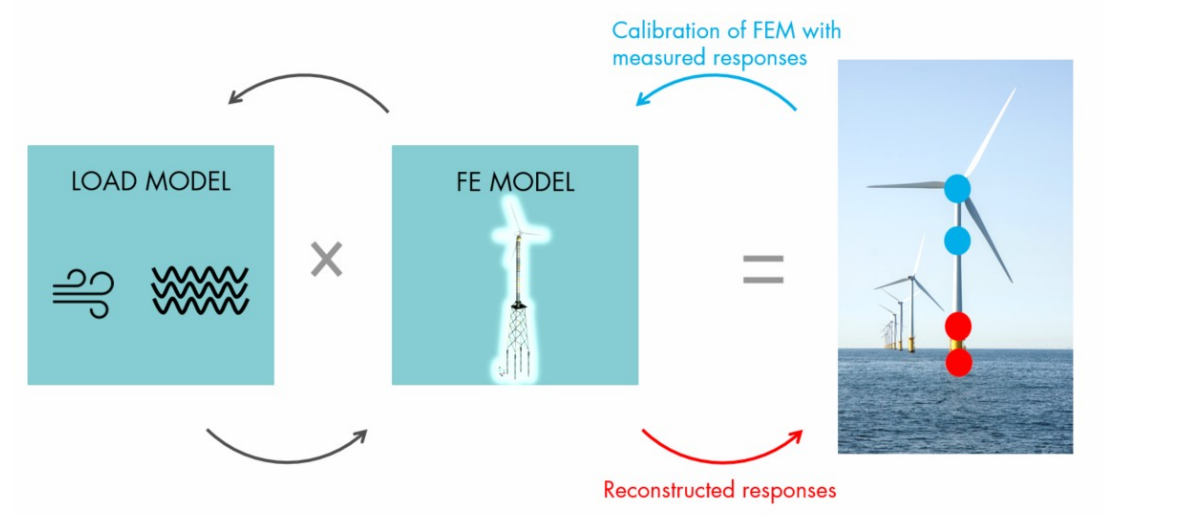

Figure 22: Interaction between the components of the prediction model used in the load reconstruction.

The load model includes the simulation of the wind and wave loads acting on the foundation structure. The level of detail of this simulation depends on the assumptions made, which in practice, are often defined by the available resources and design information. Figure 23 shows four possible load models that include a different number of internal forces (shear forces and bending moments) resulting from the acting wind and wave loads. In model 1, only the acting wind thrust is considered by a shear force acting at the height of the rotor hub. Model 2 has an better accuracy by additionally representing the moment caused by wind. Model 3 considers both wind and wave loads through concentrated shear forces and bending moments. The highest level of detail and accuracy is granted by load model 4, which considers wind and wave action as distributed loads.

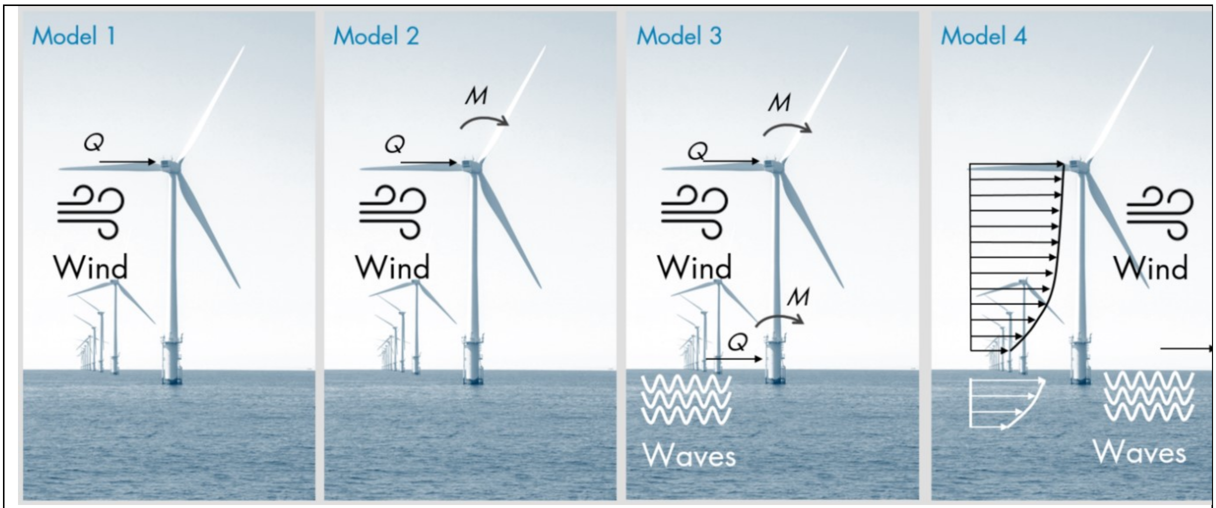

Figure 23: Load models with different assumptions regarding wind and wave loads.

Furthermore, a FE model of the entire structure is required. In the case of an offshore wind turbine with a monopile support structure, the overall structure includes the monopile, transition piece and tower, which are modelled in a simplified manned using beam elements with circular cross section. The rotor mass, the nacelle mass, the resonating water mass and other turbine-specific additional masses are integrated into the model as lumped or distributed masses. The integration of the monopile into the soil is modelled in a simplified way by single linear elastic springs. The lateral spring stiffness, the shaft stiffness and the vertical stiffness at the pile tip can be determined with an iterative calculation from the nonlinear p-y, t-z and Q-z curves of the different soil layers according to API RP 2GEO [3] (see Figure 24). After the model generation, the model is validated and updated using the measured dynamic responses so that the two first natural frequencies in the two main directions are in accordance with the measured natural frequencies.

The number of available measurement positions affects the accuracy of the prediction model, since each measurement point represents a degree of freedom and, thus, provides additional information of the actual structural response. The entire prediction model is validated and calibrated by comparing the estimated, reconstructed loads with the loads directly measured by strain sensors, as shown in section 6.2.

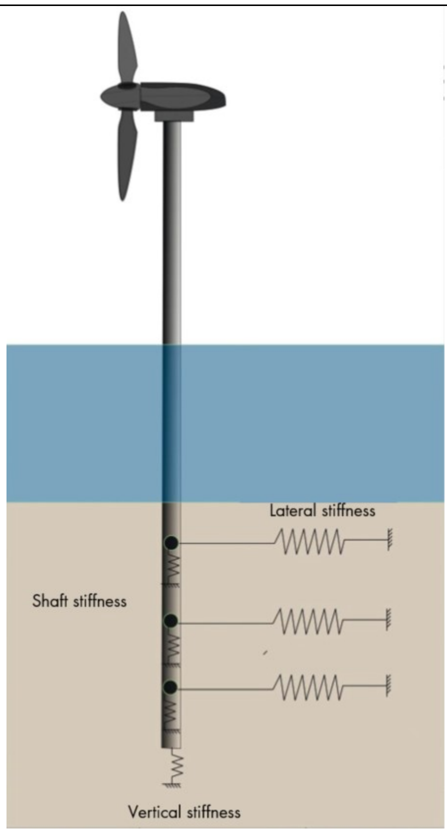

Figure 24: Illustration of the soil-structure model of an offshore wind turbine with a monopile support structure.

6.1.2. Uncertainties in the fatigue load estimation

The process of load estimation, both by direct strain data and by load reconstruction, involves some uncertainties that are introduced by various factors, such as measurement errors, calibration errors, and the load reconstruction methodology itself. Below, we provide a brief description of the some sources of uncertainties present in the used load estimation methodology:

- Measurement uncertainties:
  - Measurement uncertainties and errors caused by the sensors (e.g., amplitude and phase errors, offset drifts due to temperature and aging of accelerometers, inclinometers and strain sensors)
  - Measurement uncertainties and errors caused by the data acquisition (e.g., digitization errors, errors due to signal filters, etc.)
  - Uncertainties/errors introduced by the calibration of the sensors
- Model uncertainties:
  - Errors introduced by the deviation between the properties of the real (as-built) structure and the corresponding design assumptions (e.g., eccentricity of rotor-nacelle assembly)
  - Simplified/erroneous model assumptions, e.g., deviations from the real structure due to nonlinearities and inaccuracies in foundation stiffness
- Uncertainties of the load reconstruction approach:
  - Since the load reconstruction is based on the FE model of the structure, errors arise from the underlying load assumptions in addition to the aforementioned model uncertainties (see Figure 23).

6.2. Results and validation

The presented monitoring concept, which is based on the combination of direct load measurement and load reconstruction, is currently applied in several offshore wind farms. In this section, the results from one offshore wind farm are presented exemplarily. The structures have a monopile foundation and a TP that is connected to the tower with a flange connection. The sensor configuration for 10% of the turbines in the wind farm includes strain gauges and inclination sensors at the tower/TP connection and accelerometers at the tower top. The remaining turbines in the wind farm are also instrumented with an inclination sensor and accelerometer, but have no strain sensors.

First, the approach was validated at the turbines equipped with strain gauges. The overall structure was modelled using finite elements as described in section 6.1.1. Several prediction models were built and applied to reconstruct the loads at the tower/TP interface. The bending moments reconstructed from accelerometers, inclinometers and the FE model were compared with those directly measured from the strain gauges.

Figure 25 shows the comparison between the measured and reconstructed bending moments about the x and y axes for two prediction models. The second prediction model (lower part of Figure 25) shows a higher accuracy compared to the first prediction model (upper part of Figure 25). This is manifested, on the one hand, by an improved representation of the low-frequency components of the signal, as can be observed for the bending moments about the y-axis (M_y), and, on the other hand, by a better reconstruction of the load amplitudes. Based on the validation results, the load reconstruction model was optimized to increase the damage assessment accuracy. Subsequently, this model was transferred to all turbines of the wind farm in order to obtain a continuous evaluation of the fatigue loads and the derived DEL or fatigue damage across the wind farm.

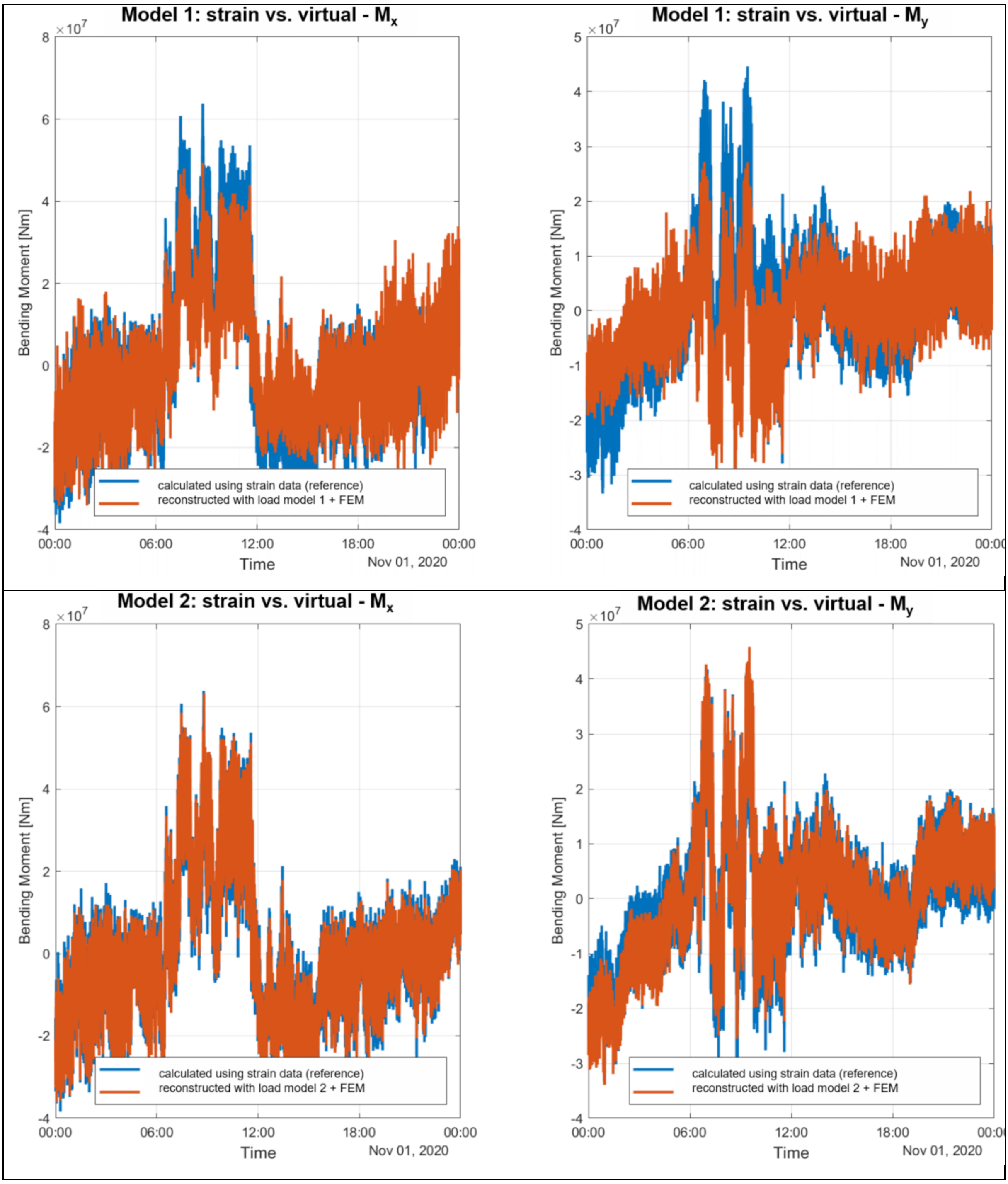

Figure 25: Comparison between measured bending moments from strain signals and reconstructed bending moments from dynamic sensor data – prediction model 1 (upper subplots) and prediction model 2 (lower subplots).

The DEL at the tower/TP connection can be used to derive the life consumption and compare the evolution of lifetime consumption to the design assumptions. In Figure 26, the evolution of lifetime consumption is presented exemplarily for three turbines of an offshore wind farm. The analyzed time period is one year and the results are shown for the bending moments about the x-axis (left subplot) and y-axis (right subplot). The fatigue life consumption was determined at twelve points, evenly distributed around the circumference of the tower cross section. The respective color-coded areas show the variance of the determined life consumption and considers all points around the circumference of the circle also taking into account uncertainties in the strain measurement or load reconstruction. The black line indicates the anticipated lifetime consumption according to design, which assumes a linear damage progression.

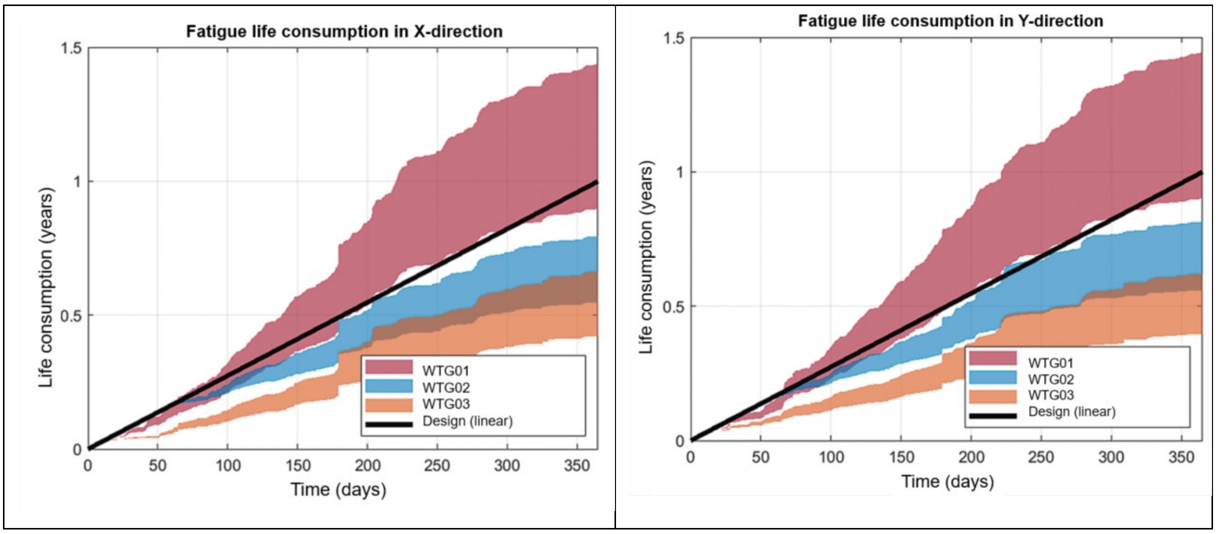

Figure 26: Evolution of fatigue life consumption in years for three wind turbines based on reconstructed loads; the black line represents the linear fatigue life consumption assumed in design

In this representation, particularly damage-relevant events are clearly indicated as vertical steps. As expected, all turbines show similar progressions, since they have neighboring locations and are exposed to similar wind and wave conditions.

Wind turbine WTG01 shows a higher lifetime consumption than assumed in design for the same period. The possible reasons behind these effects can be analyzed in further targeted investigations. Such illustrations of lifetime consumption allow a simple identification of assets that require further investigations and operational optimization.

Furthermore, it is possible to identify events with a higher damage contribution and the corresponding operating states, so that the possible causes can be narrowed down in time and measures can be taken. The investigation of the correlation between damage contribution and environmental and operational conditions provides a significant contribution to the identification of operating conditions that are fatigue-intensive and can potentially endanger the structural integrity if they occur frequently.

In Figure 27, the wind speed is plotted as a function of the generator speed and the probability density of the absolute damage contribution is indicated by the color of the data points (scaling is hidden for confidentiality reasons). This representation corresponds to the contribution to total damage over time, which was shown in Figure 26. A normalization over the frequency of occurrence provides a clear indication of which operating conditions were particularly fatigue-relevant to the structure (see upper left subplot in Figure 27). Similarly, a normalization over the density of the generated power can be performed, as shown in the lower subplot of Figure 27. In this manner, operating conditions that exhibit a particularly unfavorable relationship between structural damage and economic yield can be identified.

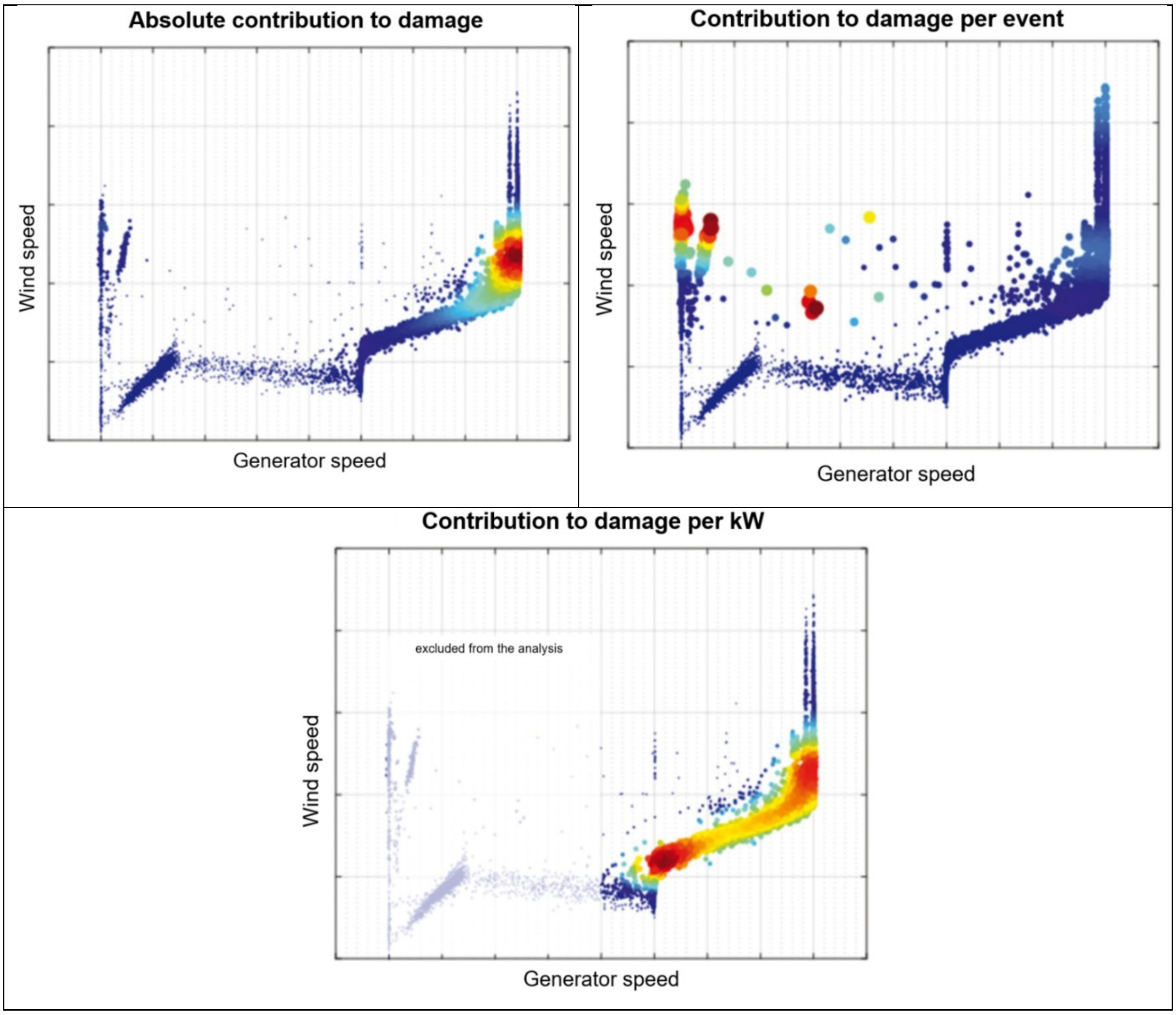

Figure 27: Absolute and relative contribution to damage as a function of the environmental and operational conditions.

6.3. Discussion

The reliable determination of fatigue loads and their assessment at wind farm level is essential for the data-driven optimization of the turbine operation and for assessing the potential life extension of foundation structures. Acting loads can be directly acquired by strain measurements. However, it is not possible to install strain sensors on multiple cross sections of the structure or at all WTGs of a wind farm due to technical and financial reasons. Alternatively, the fatigue loads can be reconstructed by exploiting the combination of measured structural responses at the tower (e.g., accelerations or inclinations) and a FE model. This process is often referred to as load reconstruction based on virtual sensors or digital twins.

Measured or reconstructed loads are used to calculate DEL, which are directly comparable with the assumptions or calculations from the structural design and are used to determine the actual fatigue damage experienced by the structures. The approach to load reconstruction presented in the chapter, does not require direct strain measurements. However, for larger offshore wind farms, it is recommended to additionally equip individual WTGs with strain sensors, in order to enable a wind farm-specific validation of the approach. This proposed approach offers an economically viable solution for fleet monitoring, i.e., for the instrumentation of all WTGs within a wind farm with a SHM system, since it deploys only data of acceleration or inclination sensors which can be installed in the tower area relatively easily, while relatively expensive strain sensors can be omitted.

The load reconstruction approach presented in this paper is currently already successfully applied in several offshore wind farms and is being continuously developed further. A good agreement between loads measured directly by strain sensors and those provided by the load reconstruction approach can also be achieved with simple load models. The associated inaccuracies in the load estimation can be quantified. Often, the fleet monitoring results regarding fatigue extracted for wind farms fully equipped with structural monitoring systems, show that lifetime consumption is not evenly distributed within the wind farm and therefore each turbine should be considered individually. The analysis of the fatigue damage evolution and the comparison among the turbines provide important information about locations with lifetime consumption that is above average, as well as about events with a high contribution to damage. Finally, suboptimal operating conditions can be identified by the correlation analysis between fatigue damage and operating and environmental conditions, yielding a recommendation for the optimization of the turbine operation.

7 Comparison

In the previous sections, four different approach for the assessment of the remaining lifetime of wind turbines have been presented. Each of the four approaches has its own advantages and limitations and is based on different data. In the following, for all four approaches, the required data, the generated output as well as the underlying assumptions and/or limitations are summarised. An overview is given in Table 9.

Generic approach (Section 3):

The generic approach presented in section 3 may provide a first line estimate of the remaining useful lifetime by drawing on publicly available turbine models together with a site-specific wind climate assessment. The method relies on a relative approach where site-specific loads are compared to the design class loads. However, due to the limited knowledge of the actual turbine information of design margins is lost and also the fatigue damage assessment is limited to the framework of damage equailent loads. The method is therefore best suited for early decision support when wind turbines approach their design lifetime and their continued operation needs to be evalauted.

Temporal extrapolation (Section 4):

For the probabilistic temporal lifetime estimation, 10 min SCADA data and high-resolution strain data is needed, as the measured strain data is used to calculate short-term fatigue values which are extrapolated to lifetime fatigue values using correlations with SCADA data. Hence, on the one hand, the amount of measurement data is relatively high compared to the other approaches presented in this work. On the other hand, data regarding the turbine itself is not required, as this approach is a simulation model-free approach. The outputs of the temporal extrapolation are actual lifetime values or damage equivalent loads at each strain gauge location. This directly illustrates the benefits and limitations of this approach. The main benefit is that this approach delivers real absolute lifetime values, as it based on strain data. This means that results are not only relative comparisons with original designs, e.g., statements like “the lifetime is 10 % higher compared to the original design”. On the downside, results are only available at the strain gauge positions. For other positions, additional spatial extrapolations are required.

Indirect lifetime estimation (Section 5):

In the indirect lifetime estimation 10-minute SCADA or met mast data and aero-servo-elastic simulations are used to reconstruct the load history and calculate lifetime fatigues for different components. Gaps in the SCADA time series can be filled by publicly available reanalysis data. Inflow conditions (including wakes) are modelled with the open-source software Floris and

TurbSim. The advantage of this approach is that it only relies on commonly available SCADA measurements or publicly available reanalysis data (such as ERA5 or NEWA) as input. For the aero-servo-elastic simulations, on the other hand, accurate turbine models must be used to obtain reliable lifetime predictions. With generic turbine models, only relative statements can be made about the service life of a turbine compared to reference turbines.

Load reconstruction (Section 6):

The load reconstruction approach presented in Section 6 offers a solution for reliable and economically viable fleet monitoring in terms of fatigue life consumption. The approach does not require direct strain measurements, but only data of acceleration and inclinations sensors installed in the tower area (tower top and possibly tower bottom or transition piece). However, for larger offshore wind farms, it is recommended to additionally equip individual WTGs with strain sensors, in order to enable a wind farm-specific validation of the approach. All input data (acceleration, inclination and strain) should have a high resolution. The output of the approach are DEL, the evolution of the fatigue life consumption and the remaining fatigue life of the individual structures at the examined critical sections. The acceleration and inclination data are exploited in conjunction with a FE model of the overall structure. Design information, such as geometrical data and material properties are required for the generation of the FE model.

10-minute averages of the SCADA data, i.e., of environmental and operational conditions (EOCs), such as yaw angle, wind speed and active power, are not a prerequisite for the deployment of the approach. However, these can be assessed in combination with the results of the load reconstruction approach to provide insight on potential correlations between fatigue damage and EOCs, identify suboptimal operational conditions and obtain recommendations for the optimization of the turbine operation.

Table 9: Comparison of lifetime assessment methods

	Required data	Generated outputs	Limitations & benefits
Generic approach (Section 3)	• Site specific wind climate • Representative generic turbine	• Lifetime estimate at selected components	• Only relative analysis possible • Enable early decision support with minimal data requriement
Temporal extrapolation (Section 4)	• 10 min SCADA data • High resolution strain data • No turbine model at all	• Actual fatigue lifetime at a measurement position	• Results only at position of the strain gauges • No model errors
Indirect lifetime estimation (Section 5)	• 10-min SCADA data • Meteorological reanalysis data • Aeroelastic turbine model	• Lifetime fatigue	• Accuracy dependent on input data and turbine model • Lifetime fatigue for arbitrary components of the turbine
Load reconstruction (Section 6)	• High resolution acceleration or inclination data (e.g., at 90% of the farm turbines) • Stiffness of the overall structure. Either extracted from a FE model (design information required) or determined experimentally (less detailed design information required) • High resolution strain data (optionally at 10% of the farm turbines for validation purposes) • 10 minute SCADA data (optional for investigation of correlations)	• DEL, evolution of fatigue life consumption and remaining fatigue life at critical sections (e.g., at tower/TP interface) • DEL and remaining fatigue life at sections equipped with strain gauges (e.g., at tower/TP interface)	• Validation only possible if some turbines in the wind farm are equipped with strain gauges • Design information required • Enabling reliable fleet monitoring with a low amount of sensors and at viable cost.

8 Conclusion

The work presented in this deliverable contributes to work package 1 of the IEA Wind Task 42 on wind turbine lifetime extensions. The overall objectives of this work package are the development and evaluation of methods for reliability and safety assessments. This deliverable focusses on fatigue lifetime predictions for lifetime extension. It covers two tasks: 1) data-driven methods for remaining lifetime assessments and 2) the value of data in the context of remaining lifetime assessments.

For the first task, various methods are development (Section 3 to 6) and compared. A complete benchmark using the same data set was not conducted. This has several reasons, inter alia, the different types of data required by the various approaches and the unavailability of high-quality open-access data. Hence, the comparison focussed on more general aspects like the required data, resulting model outputs and benefits & limitations. Details regarding the comparison are summarised in Section 7. In a nutshell, it is shown that additional data allow a more thorough remaining lifetime estimation and, therefore, have an additional value. Whether this additional value justifies higher computation times or additional costs due to more advanced measurements cannot be answered here and might be project dependent.

The second task focusses on the value of data itself. First, data which might be relevant for lifetime assessments have to be classified. Second, the value of such data must be analysed by comparing possible outputs and limitation of different methods. In general, relevant data can be divided into three classes: SCADA/ meteorological data, strain/acceleration data and turbine design data. If only SCADA data are available, it is possible to estimate the remaining lifetime using generic turbine models (cf. Section 3). However, these methods depend on the similarity of the generic turbine model with the turbine at question and are more suitable for early-stage remaining lifetime assessments. If SCADA and strain data are available, highly accurate predictions are possible without the usage of a turbine model (cf. Section 4). On the downside, these predictions are limited to those components/sections for which strain data are available. Finally, if all three types of data are available, predictions for all critical components are possible (cf. Section 5 & 6). Hence, to conclude, additional data does enable more advanced remaining lifetime assessments. Whether the use of more data is cost-efficient cannot be judged based on the present work.

References

Bak, C., Zahle, F., Bitsche, R., Kim, T., Yde, A., Henriksen, L., . . . Hansen, M. H. (2013). *Description of the DTU 10 MW Reference Wind Turbine.* DTU Wind Enerfy Report-I-0092.

Braunbehrens, R., Vad, A., & Bottasso, C. L. (2022). The wind farm as a sensor: learning and explaining orographic and plant-induced flow heterogeneities from operational data. *Wind Energ. Sci. (Wind Energy Science)*.

d N Santos, F., Noppe, N., Weijtjens, W., & Devriendt, C. (2022). Data-driven farm-wide fatigue estimation on jacket-foundation OWTs for multiple SHM setups. *Wind Energ. Sci., 7*, 299–321.

DNVGL-ST-0262. (2016). *Lifetime extension of turbines.*

Hübler, C., & Rolfes, R. (2022). Probabilistic temporal extrapolation of fatigue damage of offshore wind turbine substructures based on strain measurements. *Wind Energ. Sci., 7*, 1919-1940.

Hübler, C., Weijtjens, W., Rolfes, R., & Devriendt, C. (2018). Reliability analysis of fatigue damage extrapolations of wind turbines using offshore strain measurements. *J. Phys.-Conf. Ser., 1037*, 032035.

IEC. (2019). *International Standard IEC 61400-1 ed. 4, Wind Turbines - Part 1 Design Rquirements.*

Jonkman, J. (2015). *FAST an aeroelastic computer-aided engineering (CAE) tool for horizontal axis wind turbnines*. Retrieved from https://nwtc.nrel.gov/FAST

Jonkman, J. M., & Shaler, K. (2021). *Fast. farm user's guide and theory manual.* National Renewable Energy Laboratory Golden, CO.

Jonkman, J., Butterfield, S., Musial, W., & Scott, G. (2009). *Definition of a 5-MW Reference Wind Turbine for Offshore System Development.* NREL/TP-500-38060.

Jourdier, B. (2020). Evaluation of ERA5, MERRA-2, COSMO-REA6, NEWA and AROME to simulate wind power production over France. *Adv. Sci. Res. (Advances in Science and Research)*, 63–77.

Lee, J., & Zhao, F. (2022). *GWEC: Global Wind Report 2022.* Global Wind Energy Council. Retrieved from https://gwec.net/global-wind-report-2022/

Loraux, C., & Brühwiler, E. (2016). The use of long term monitoring data for the extension of the service duration of existing wind turbine support structures. *J. Phys.-Conf. Ser., 753*, 072023.

Marsh, G. (2016). *Fatigue load monitoring of offshore wind turbine support structures.* Doctoral dissertation, University of Strathclyde.

Megavind. (2016). *Strategy for Extending the Useful Lifetime of a Wind Turbine.*

Noppe, N., Hübler, C., Devriendt, C., & Weijtjens, W. (2020). Validated extrapolation of measured damage within an offshore wind farm using instrumented fleet leaders. *J. Phys.-Conf. Ser., 1618*, 022005.

NREL. (2021). *FLORIS. Version 2.3.0.*

Paulsen, U. S., Gomiero, M., Larsen, T. J., & Benini, E. (2018). Load validation of aero-elastic simulations with measurements performed on a 850 kW Horizonthal axis wind turbine. *IOP conf. Series. : Journal of Physics: Conf. Series 1037*, 062023.

Peña, A., Mann, J., & Rolighed Thorsen, G. (2018). *DTU Wind Energy E Vol. 0177 : SpinnerLidar measurements for the CCAV52.* Technical University of Denmark , DTU Wind Energy . DTU Wind Energy. Retrieved from https://backend.orbit.dtu.dk/ws/portalfiles/portal/193377980/Report_with_cover.pdf

Rinker, J. M., Hansen, M. H., & Larsen, T. J. (2018). Calibrating a wind turbine model using diverse datasets. *IOP Conf. Series: Journal of Physics: Conf. Series 1037*, 062026.

Rinker, J., & Dykes, K. (2018). *WindPACT Reference Wind Turbines.* NREL/TP-5000-67667.

Soltani, M. N., Knudsen, T., Svenstrup, M., Wisniewski, R., Brath, P., Ortega, R., & Johnson, K. (2013). Estimation of Rotor Effective Wind Speed: A Comparison. *IEEE Trans. Contr. Syst. Technol. (IEEE Transactions on Control Systems Technology)*, 1155–1167.

Tsiapoki, S., Colomer Segura, C., & Ebert, C. (2. May 2022). Schwingungsbasierte Lastrekonstruktion an Gründungsstrukturen von Offshore-Windenergieanalagen. *Bautechnik*, S. 8. doi:https://doi.org/10.1002/bate.202200037

VDI. (2020, 01). *Structure monitoring and assessment of wind turbines and offshore stations*.

Ziegler, L., Cosack, N., Kolios, A., & Muskulus, M. (2019). Structural monitoring for lifetime extension of offshore wind monopiles: Verification of strain-based load extrapolation algorithm. *Mar. Struct., 66*, 154–163.